IEEE Access
Multidisciplinary | Rapid Review | Open Access Journal

Received 20 January 2023, accepted 10 February 2023, date of publication 16 February 2023, date of current version 23 February 2023.

Digital Object Identifier 10.1109/ACCESS.2023.3246108

RESEARCH ARTICLE

Machine Learning Prediction Based Adaptive Duty Cycle MAC Protocol for Solar Energy Harvesting Wireless Sensor Networks

SOHAIL SARANG[1], (Graduate Student Member, IEEE), GORAN M. STOJANOVIĆ[1], (Member, IEEE), MICHEAL DRIEBERG[2], (Member, IEEE), STEVAN STANKOVSKI[1], (Member, IEEE), KISHORE BINGI[2], (Member, IEEE), AND VARUN JEOTI[1], (Senior Member, IEEE)

[1]Faculty of Technical Sciences, University of Novi Sad, 21000 Novi Sad, Serbia
[2]Department of Electrical and Electronic Engineering, Universiti Teknologi PETRONAS, Seri Iskandar, Perak 32610, Malaysia

Corresponding author: Sohail Sarang (sohail@uns.ac.rs)

This work was supported by the European Union's Horizon 2020 Research and Innovation Programme under the Marie Skłodowska-Curie Grant under Agreement H2020-MSCA-ITN-2018-813680.

ABSTRACT The dynamic nature of energy harvesting rate, arising because of ever changing weather conditions, raises new concerns in energy harvesting based wireless sensor networks (EH-WSNs). Therefore, this drives the development of energy aware EH solutions. Formerly, many Medium Access Control (MAC) protocols have been developed for EH-WSNs. However, optimizing MAC protocol performance by incorporating predicted future energy intake is relatively new in EH-WSNs. Furthermore, existing MAC protocols do not fully harness the high harvested energy to perform aggressively despite the availability of sufficient energy resources. Therefore, a prediction-based adaptive duty cycle (PADC) MAC protocol has been proposed, called PADC-MAC, that incorporates current and future harvested energy information using the mathematical formulation to improve network performance. Furthermore, a machine learning model, namely nonlinear autoregressive (NAR) neural network, is employed that achieves good prediction accuracy under dynamic harvesting scenarios. As a result, it enables the receiver node to perform aggressively better when there is sufficient inflow of incoming harvesting energy. In addition, PADC-MAC uses a self-adaptation technique that reduces energy consumption. The performance of PADC-MAC is evaluated using GreenCastalia in terms of packet delay, network throughput, packet delivery ratio, energy consumption per bit, receiver energy consumption, and total network energy consumption using realistic harvesting data for 96 consecutive hours under dynamic solar harvesting conditions. The simulation results show that PADC-MAC provides lower average packet delay of the highest priority packets and all packets, energy consumption per bit, and total energy consumption by more than 10.7%, 7.8%, 81%, and 76.4%, respectively when compared to three state-of-the-art protocols for EH-WSNs.

INDEX TERMS Machine learning, solar energy prediction, adaptive duty cycle, energy harvesting aware communication, MAC protocol, EH-WSNs.

I. INTRODUCTION

Nowadays, the Internet of Things (IoT) is gaining strong attention in many applications, including healthcare and smart cities [1]. Wireless sensor network (WSN) plays an essential role in IoT and is widely used in different applications, such as environmental and industrial monitoring, agriculture, and others [2], [3], [4]. Conventionally, WSNs consist of several sensing nodes powered by small non-rechargeable batteries that can gather the data and direct it to the sink node, called battery-powered WSNs (BP-WSNs). However, these nodes have limited battery capacity and thus need to be

The associate editor coordinating the review of this manuscript and approving it for publication was Vicente Alarcon-Aquino.

replaced regularly, which hinders their operation and network performance. Therefore, energy efficiency remains critical to ensuring the sustainable operation of nodes [4]. For instance, schemes developed in [4] and [5] improve energy efficiency to enhance the lifetime.

In recent years, energy harvesting (EH) techniques have gained intense attention to power sensor nodes using energy sources (e.g. solar, wind, mechanical, radio frequency (RF), and thermal) [6]. For example, solar harvesting uses solar cells to collect external energy from the sun. This provides high conversion efficiency and power density [7], which have led to widespread adoption [8]. On the other hand, wind harvesting incorporates the wind turbine to harvest energy [9]. In mechanical harvesting, energy is obtained by using pressure, motion of objects, and human activity [10]. Similarly, RF harvesting is also widely utilized to generate energy from electromagnetic waves [11]. Moreover, thermal harvesting is achieved using the temperature difference between two junctions of semiconductors or the same metals [12]. Among these sources, solar has higher power density and is widely adopted in EH-WSNs [7]. Moreover, it is found that solar provides sufficient harvested energy to recharge energy storage device to the maximum capacity and also an excess energy in actual EH-WSNs. Therefore, integrating these sources with WSNs has motivated researchers to develop EH-WSNs, where, nodes can harvest energy using energy sources. This helps to mitigate the energy problem of conventional WSNs and reduce the negative environmental impact and cost of battery replacements. Furthermore, EH enables nodes to schedule tasks such as prioritization, duty cycle, and sensing, according to harvested energy profile to maximize the network performance.

The MAC protocol regulates the access of a common medium among the sensor nodes. In EH-WSNs, MAC protocols aim to optimize the network performance using harvested energy efficiently. The existing protocols incorporated the harvested energy information into settings for duty cycle, access probability, traffic load, relay node selection, and sensing interval to enhance network performance. However, in certain circumstances, for example, harvesting energy varies significantly according to the weather, which may hinder the execution of ongoing tasks and node operation. Thus, it is essential to know about the future incoming energy to avoid disruption in the node's operation during periods of energy scarcity. Furthermore, knowing the future harvested energy, the node can further optimize the performance as in the case when it has a higher energy value than required for the task execution.

Machine learning (ML) involves computer algorithms to learn automatically from data without being explicitly programmed [13]. It has gained significant attention in academia and industry and is considered a vital tool in developing automated IoT applications. In WSNs, ML techniques have been broadly used to solve various challenges such as MAC, QoS, routing, localization, data integrity and fault detection, synchronization, and data aggregation [14]. Moreover, these techniques have been used to forecast the energy at a given time slot [15], [16]. Furthermore, regression and Q-learning techniques have been used to forecast future energy in WSNs [7], [17]. Authors in [18] compared artificial neural network (ANN) based ML models that take different parameters such as rain, time, and atmospheric pressure to forecast daily solar intensity. Therefore, predicting future harvested energy enables the development of harvesting aware solutions, such as communication protocols [19]. Moreover, it can further help optimize MAC protocols to enhance network performance [13].

A. MOTIVATION

Recently, EH mechanisms have gained significant attention for powering up sensor nodes. This drives the design of EH aware schemes to enhance the performance using the harvested energy [6], [20]. Because of this, numerous MAC protocols have been proposed for EH-WSNs [11]. However, most of the existing receiver-initiated MAC protocols lack smart energy allocation strategies such as adaptive duty cycling mechanism. Without smart energy allocation strategies, the dynamic harvesting conditions may affect ongoing node operation and degrade network performance, especially during periods of energy scarcity. In certain circumstances, for example, on a typical sunny day, these protocols may not be able to perform aggressively since the next day may turn out to be a rainy day. Therefore, data packets suffer long delays despite sufficient energy resources. In addition, these protocols do not plan how to optimize performance when the harvested energy value is greater than or equal to the energy required for the task execution. Furthermore, these protocols do not have any plans on how to take advantage of the utilization of the surplus future harvested energy in high harvesting conditions, which leads to energy wastage. Furthermore, most available protocols have not been tested using actual solar irradiance. Also, their performance evaluation did not include most performance metrics such as end-to-end (E2E) delay, network throughput, packet delivery ratio (PDR), energy consumption per bit, receiver energy consumption, and total network energy consumption.

Therefore, there is a need to develop a novel and more realistic adaptive MAC protocol that can adapt the node operation according to dynamic solar irradiance scenarios and can use excess harvested energy in devising smart energy allocation strategies to enhance the network performance. Furthermore, predicted incoming energy is incorporated to improve the network performance. Moreover, the performance of the protocol and comparison with state-of-the-art protocols for EH-WSNs, is evaluated comprehensively under a realistic scenario using actual harvesting rates. The performance metrics include E2E delay, PDR, network throughput, energy consumption per bit, receiver energy consumption, and total network energy consumption.

B. MAIN CONTRIBUTIONS

The contributions of this work are as follows:

- The proposed Prediction based Adaptive Duty Cycle MAC (PADC-MAC) protocol introduces a numerical formula to set the duty cycle according to the predicted incoming harvested energy.
- ML model is developed to predict the incoming harvesting energy, which enables the receiver node to perform more aggressively when it has a sufficient inflow of incoming harvested energy to improve the performance.
- A technique by which the receiver shares its next duty cycle with all senders that optimizes their sleep duration, resulting in energy efficiency improvements.
- The performance of PADC-MAC is evaluated using GreenCastalia for four consecutive days, i.e., 96 hours of simulation using actual harvesting rates under high and low solar irradiance conditions.
- The performance of PADC-MAC is compared with QPPD-MAC, QAEE-MAC, and EEM-MAC.
- The results indicate that the PADC-MAC provides better performance in terms of E2E delay, energy consumption per bit, and total network energy consumption when compared to three state-of-the-art MAC protocols for EH-WSNs.

C. ORGANIZATION

The remainder of this paper is organized as follows: Section II comprehensively describes the importance of energy prediction in EH-WSNs. Then, previous works on MAC protocols and their classification are given in detail. Section III describes the PADC-MAC protocol. First, the communication overview of PADC-MAC is presented. Furthermore, it presents the prediction model, named NARNET model. Then, a mathematical formula is proposed that sets the receiver duty cycle, which corresponds to the current and expected incoming harvested energy obtained using the prediction model. In addition, the results of an investigation have been provided to find an optimal range of energy and its impact on the performance. Next, the self-adaptation technique is explained. Section IV explains the energy model and performance metrics for evaluation. Section V presents the simulation setup and network topology used in the performance evaluation. Then, the performance results of the proposed NARNET model and its comparisons with EWMA and actual data under dynamic harvesting conditions, are given. Next, the performance evaluation of the PADC-MAC protocol using GreenCastalia, which incorporates energy prediction results obtained using NARNET, is presented. Finally, the performance comparison with three well-known protocols under high and low EH conditions, is discussed in detail. Section VI concludes the paper and provides the future work.

II. RELATED WORK

A. ENERGY PREDICTION IN EH-WSNs

In EH-WSNs, the dynamic harvesting conditions drives to design smart and reliable energy allocation strategies while considering the EH conditions. For example, for EH source such as mechanical, the EH process is typically unpredictable. This provides the motivation to develop scheduling schemes that do not have statistical knowledge about the EH process for data transmission. To address this issue, authors in [21] have proposed a uniforming random ordered policy, named UROP, that enables the fusion center to schedule the transmission time for each sender node without knowing about the EH process and battery capacity of the node. The developed approach helps to perform data transmission using the information of previous transmission attempts. The results show that, it reduces the data backlogs while achieving nearly optimal throughput over finite time horizons in EH-WSNs. In [22], authors have used the Markov decision process (MDP) to maximize the energy utilization to find an optimal task scheduling such as sensing and packet transmission for the node. Moreover, an energy aware scheduling algorithm has been proposed that employs MDP to optimize reliability in EH-WSNs [23]. On the other hand, solar harvesting has been widely in considered literature, and its energy can be forecasted based on past energy patterns. This drives the development of new schemes which may provide enough knowledge about the incoming harvesting energy to avoid any disruption in current node operation and allocate future tasks accordingly [6]. By estimating the future harvesting energy, the node can exploit the expected available energy at best by introducing smart strategies based on energy profile to enhance the network performance. Furthermore, this information can also help nodes to schedule their current operation in such a way that operations can be sustained during periods of energy scarcity. Formerly, several energy prediction schemes have been designed to predict the incoming harvesting energy from solar EH. They can be used to forecast the incoming energy that can be utilized to devise EH aware schemes, such as protocols, adaptive load distribution, and others [19].

Exponential weight moving average (EWMA) [24] considers that the available energy at a specific day slot is similar to the previous days. It maintains the energy profiles of past days and utilizes that information to forecast the energy for the next time slot. Therefore, EWMA provides good prediction results for long-term seasonal conditions. Weather conditioned moving average WCMA [25] predicts the future energy intake by incorporating the weather conditions and harvested energy of the present and previous days. Specifically, a matrix is used to store energy intake values. Q-learning-based solar energy prediction (QLSEP) [7] addresses the shortcomings of EWMA which is suitable for long-term seasonal conditions. It considers past energy profiles as well as weather variations to forecast energy intake in a particular slot. Pro-Energy [26] uses the energy profiles of previous days as other models to forecast future energy intake. It maintains the harvested energy profiles of past days such as cloudy, sunny, and rainy, and incorporates past values to estimate the energy intake in the next slot. Enhanced-Pro [19] utilizes real-life solar traces to predict future intake. The model introduces two factors:

fine adjustment index and tuning factor for better prediction accuracy. It involves past energy profiles as Pro-Energy to calculate a correlation coefficient factor using the current harvested energy profile. However, most of these models do not perform well when sudden changes occur in weather conditions and provide significant errors when employed in dynamic conditions (e.g., sunny, partially sunny, consecutive cloudy days). Furthermore, the effectiveness of these models at the MAC layer has gained little consideration that can help in designing adaptive schemes based on predicted energy to improve performance [19].

B. MAC PROTOCOLS FOR EH-WSNs

In EH-WSNs, MAC protocols aim to utilize the gathered energy efficiently to enhance performance [27]. Formerly, numerous MAC protocols have been developed, that account the harvested energy in scheduling various tasks e.g. duty cycle. Furthermore, these protocols can be divided into three categories based on the initiation process, namely sender, sink, and receiver initiated approaches [28].

In sender-initiated schemes such as DeepSleep-MAC [29], EL-MAC [30], SEHEE-MAC [31], EA-MAC [32], and HA-MAC [33], the sender sends a short preamble to begin the communication process. On the other hand, the receiver will be able to receive the preamble after waking up. Then, it replies with an acknowledgment (ACK) and listens to the channel for the data packet. Examples of sink-initiated protocols are AE-MAC [34], REE-MAC [35], E-MAC [36], S-LEARN-MAC [37], CEH-MAC [38] and others [28]. In these protocols, the sink initiates communication by broadcasting a packet that indicates data communication.

The receiver-initiated protocols are widely used in EH-WSNs and achieve better performance than others [39]. They include HM-RIMAC [40], EH-MAC [41], OD-MAC [42], LEB-MAC [43], MDP-SHE-WSNS [44], ERI-MAC [45], HAS-MAC [46], QAEE-MAC [47], ED-CR [48], PBP-MAC [49], SyWiM-MAC [50], R-MAC [51], EH-TDMA-MAC [52], EEM-MAC [53], RF-AASP-MAC [54], ENCOD-MAC [55], QPPD-MAC [56] and PSL-MAC [57]. In these protocols, the receiver starts the communication by broadcasting a beacon that informs all senders to transmit data packets. Moreover, they incorporate harvested energy to adjust different parameters. For example, HM-RIMAC [40] enables nodes to adjust their wake-up time according to energy level, and the node starts listening when enough energy is available. EH-MAC [41] incorporates the harvesting rate to regulate the access probability that decides whether to send the data packet or not. In OD-MAC [42], the receiver wakes up and uses the beacon to announce its availability toto accept the data packets. It incorporates the harvested energy to set the wake-up beacon and sensing time. LEB-MAC [43] achieve the energy and load balancing state among nodes. In MDP-SHE-WSNS [44], nodes send data packets by considering the energy level. ERI-MAC [45] uses a packet concatenation technique to enhance energy efficiency. HAS-MAC [46] adjusts the working schedule of the node according to its energy level.

In QAEE-MAC [47], the receiver adjusts medium access according to energy level and supports the packet priority. ED-CR [48] considers residual energy and accounts for the prospective increase in energy level to adjust the duty cycle of the node. PBP-MAC [49] assigns a priority to intermediate nodes based on the current harvesting rate and residual energy. SyWiM-MAC [50] uses a technique to support nodes that are powered by periodic energy sources. R-MAC [51] chooses the cluster head based on the remaining energy level or the size of data queue lengths. EH-TDMA-MAC [52] adjusts wake-up schedules according to available energy. EEM-MAC [53] regulates the duty cycle based on the remaining energy level. RF-AASP-MAC [54] adjusts the sleeping period according to traffic conditions and residual energy. ENCOD-MAC [55] incorporates the ENO condition and uses it to regulate the duty cycle to improve performance. QPPD-MAC [56] incorporates the priority of packets and adjusts the duty cycle based on different energy levels. PSL-MAC [57] employs a data accumulation processing mechanism and helps low-energy relay nodes to forward data packets.

However, the majority of available receiver-initiated MAC protocols lack smart energy allocation strategies such as energy prediction based adaptive duty cycling mechanism. Hence, there is a great need to propose a more realistic energy prediction-based MAC protocol that can incorporate the future energy intake in devising smart strategies to enhance the network performance.

III. PADC-MAC PROTOCOL FOR EH-WSNS

The development of receiver-initiated PADC-MAC protocol is described in this section. The aim is to develop an adaptive duty cycle MAC Protocol for EH-WSNs that can incorporate current and future energy intake to optimize the network performance and ensure sustainable operation under dynamic harvesting conditions. The essential parts of PADC-MAC are basic communication overview and traffic differentiation, an energy prediction model, adaptive duty cycle management, and a self-adaptation technique.

A. BASIC COMMUNICATION OVERVIEW AND TRAFFIC DIFFERENTIATION

The essential communication between the receiver and three sender nodes is shown in Figure 1. The receiver wakes up periodically and transmits a beacon, named wake-up beacon (WB). The WB aims to announce to the senders that the receiver is available to accept the packets. Furthermore, it contains duty cycle (d_c) and source address (SA), as given in Figure 2. After broadcasting WB, it initiates a waiting timer (T_w) and waits for the Tx beacon from senders. The short interframe space ($SIFS$) is the time taken by a node to switch its radio and process the packet.

PADC-MAC offers traffic differentiation to support applications that generate packets of different urgency (e.g., fire alert vs. periodic temperature measurement).

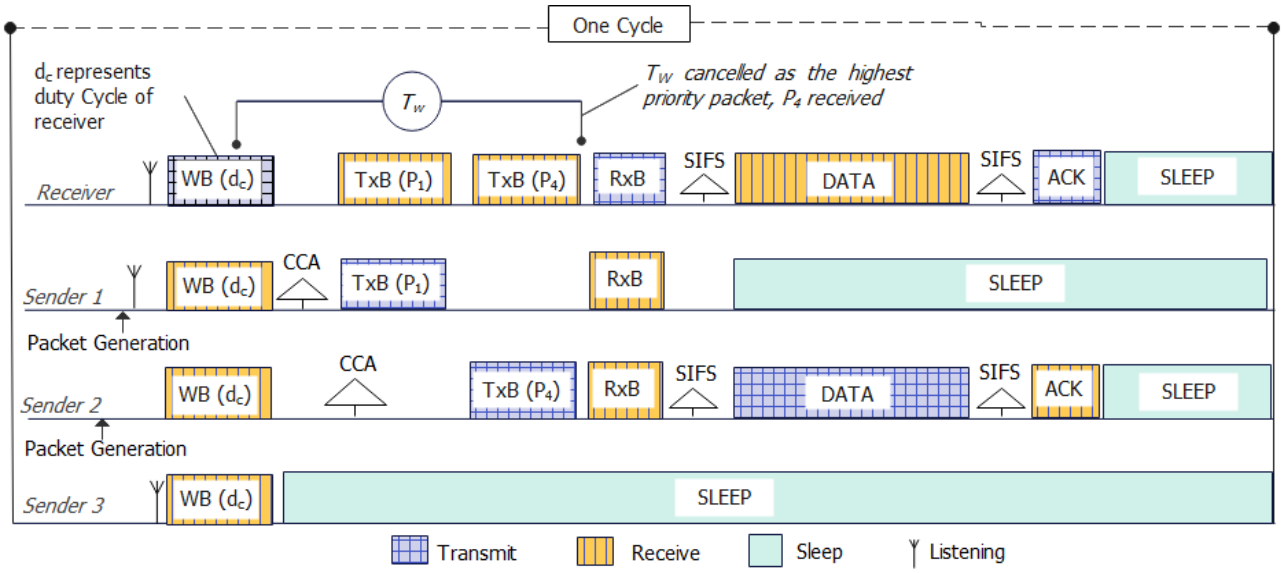

FIGURE 1. Communication overview of PADC-MAC protocol.

Thus, it allows sender nodes to assign four priority levels to data packets as normal (P_1), important (P_2), most important (P_3), and urgent (P_4). The priority assigned corresponds to the data type defined in Table 1. Upon the reception of WB, the senders perform clear channel assessment (*CCA*) and transmit Tx beacons that include the packet priority, as given in Figure 3. In contrast, the receiver collects Tx-beacon(s) and selects the sender after checking the priority field received in Tx beacons. Then, it cancels T_w accordingly. After that, it sends the Rx beacon that includes, addresses of the selected sender (*SS*) and source, and network allocation vector (*NAV*), as given in Figure 4. The Frame Check Sequence (FCS) and Frame Control (FC) are fields from IEEE 802.15.4 standard.

After receiving the Rx beacon, the chosen node immediately transmits its data packet and listens for the ACK while non-selected nodes go to sleep to preserve energy.

FIGURE 2. Frame structure of WB.

FIGURE 3. Frame structure of Tx-Beacon (TxB).

FIGURE 4. Frame structure of Rx-Beacon.

B. ENERGY PREDICTION MODEL

The EH rate varies significantly over time due to dynamic weather and seasonal changes [58]. Hence, there is a need to address the dramatic changes in harvesting energy and devise energy-aware strategies to optimize performance. Therefore, the ANN model, namely the nonlinear autoregressive neural network (NARNET), is developed that uses the past solar irradiance data to forecast future harvested energy correctly. The aim is to incorporate the information of expected incoming energy with the proposed PADC-MAC to proactively plan the available energy resources to enhance the network performance. The energy prediction mechanism involves data preparation and model development.

TABLE 1. Priority level.

Data type	Priority	Example
Urgent	P_4	Emergency alarm
Most important	P_3	Real time
Important	P_2	On-demand
Normal	P_1	Periodic

The data preparation involves raw data processing and conversion into meaningful form before training and testing data. It begins with collecting actual solar irradiance data from National Renewable Energy Laboratory (NREL), which provides high-resolution open-source irradiance data. The data contains 13862 samples of hourly solar irradiance for 19 months from April 1, 2010, to October 31, 2011, which incorporates both summer and winter data. These datasets are divided into 80% for training and 20% for testing to validate the model performance.

The structure of the proposed prediction model is given in Figure 5. The model comprises an input layer, a hidden layer, and an output layer. The hidden layer consists of ten nodes and uses *tansig* activation function to transform data into the output layer. The number of hidden layer nodes is chosen as 10 through the trial-and-error procedure to obtain

good accuracy while considering model complexity and computation time. Furthermore, the hidden layer takes the weight and bias parameters to manage neurons. In this perspective, the learning aims to find optimal weight values that provide the minimum error. For that, the model incorporates the Levenberg–Marquardt algorithm for weight adaptation. The output layer involves one node and uses pure linear (*purelin*) activation to forecast the energy in the next slot. Table 2 describes the notations used in the model structure. The NARNET model can be written using Eq. (1) [59].

$$y(t) = h(y(t-1), y(t-2), .., y(t-p)) + \epsilon(t) \quad (1)$$

where $y(t)$ represents the predicted value of data series y at time t using p past values. The function $h(*)$ is unknown in advance and is approximated through the optimization of weights and neuron bias, and $\epsilon(t)$ indicates the error obtained from the model at time t.

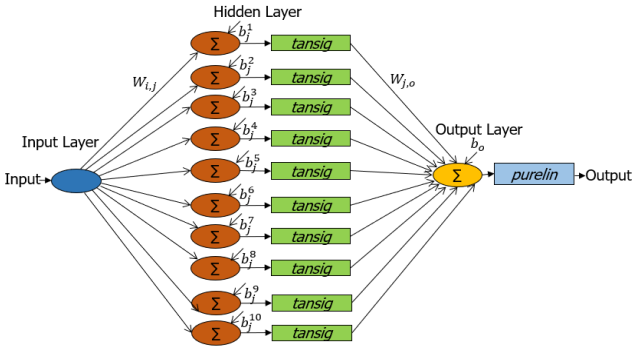

FIGURE 5. Structure of proposed neural network model with ten hidden layer nodes.

TABLE 2. Notations used in the structure of the neural network.

Notation	Description
$W_{i,j}$	Weights between input node i and hidden node j
b_j	Bias at hidden node j
tansig	Tangent sigmoid activation function
$W_{j,o}$	Weights between hidden node j and output node o
b_o	Bias at output node o
purelin	Pure linear activation function

C. ADAPTIVE DUTY CYCLE MECHANISM

The dynamic EH conditions lead to uncertainty in the available energy, which drives the development of an adaptive duty cycle mechanism to ensure sustainable operation, specifically during periods of energy scarcity. Furthermore, increasing the duty cycle when energy is abundant improves the network performance. In addition to the adaptable duty cycle, the node incorporates an additional feature that allows it to consider the incoming harvested energy to enhance the network performance further. This feature addresses the energy's unpredictable nature and enables nodes to use this knowledge to plan the available energy resources. Therefore, PADC-MAC supports the adaptive duty cycle (d_c) of the receiver and adjusts its d_c based on the current energy level and the predicted energy in the next slot as follows

$$RE_{expect} = RE_{current} + E_{Predict} \quad (2)$$

where RE_{expect}, $RE_{current}$ and $E_{Predict}$ are the total expected remaining energy, current remaining energy level, and predicted energy. These values are given in joules and computed at the beginning of the slot.

TABLE 3. Duty cycle adjustment based on RE_{expect} and $E_{Predict}$.

RE_{expect} and $E_{Predict}$	d_c
$50\% \leq RE_{expect} \leq 100\%$	1
$RE_{expect} \geq 30\%$ and $E_{Predict} \geq E_c$	1
$10\% \leq RE_{expect} < 50\%$	0.11-0.55 (using Eq.(5))
$0 < RE_{expect} < 10\%$	0.05

The RE_{expect} in percentage is given as follows

$$RE_{expect} = \frac{RE_{expect}}{E_{max}} \times 100 \quad (3)$$

where E_{max} denotes the maximum battery capacity in joules. The predicted energy $E_{Predict}$ is computed using the following formula

$$E_{Predict} = S_p \times P_s \times P_e \times d_s \quad (4)$$

where S_p, P_s, P_e and d_s denote predicted solar irradiance (W/m^2) obtained from the prediction model, solar panel size (m^2), panel efficiency, and duration of each timeslot.

Table 3 shows the d_c value according to RE_{expect} and $E_{Predict}$.

In case when RE_{expect} ranges between 10% to 50%, d_c value is computed as follows

$$d_c = \frac{RE_{expect} - E_{th} + 10}{E_{max} - E_{th}} \quad (5)$$

where E_{th} is threshold energy (10%) and is applied to prevent complete battery depletion.

In Table 3, E_c denotes the energy consumption of a node when it operates at the maximum duty cycle, i.e., 1, continuously for one hour, and is computed as follows

$$E_c = (n_s \times (e_S + e_l + e_B + e_w + e_{slp})) + (n_{ds} \times N_s \times (e_{RB} + e_d + e_{ack})) \quad (6)$$

where n_s represents the number of listening slots in one hour in which no data transmission is performed. n_{ds} denotes the number of slots in which the receiver node received data packets from N_s sender nodes. e_S, e_l, e_B, e_w, and e_{slp} represent energy spent by the receiver switching its radio states, listening to the channel, sending WB beacon, waiting for Tx beacons, and in sleeping state. e_{RB}, e_d, and e_{ack} denote energy consumed in sending the Rx beacon, receiving a data packet, and transmitting an ACK packet.

The following equation can be used to calculate the sleep duration (T_{sleep}) of the node

$$T_{sleep} = \frac{T_{listen} \times (1 - d_c)}{d_c} \quad (7)$$

where T_{listen} represents the total listening time.

D. INVESTIGATION ON THE EFFECT OF UPPER RANGE OF RE_{expect}

An investigation has been conducted to find an optimal range of RE_{expect} and its impact on the performance. In the investigation, we set different upper ranges of RE_{expect} (20%, 30%, 40%, 50%, 60%, 70%, 80%, 90%), and calculated their effect on average packet delay and minimum remaining energy level of battery (in low irradiance scenario). Figure 6 and Figure 7 show the average E2E packet delay and minimum remaining energy level of the battery, respectively. It can be seen that by increasing the upper range of RE_{expect}, the average packet delay increases, but a correspondingly higher level of minimum remaining energy is obtained. However, when the upper range is above 50%, both packet delay and minimum remaining energy level remain stable. In contrast, when RE_{expect} range is below 50%, the delay performance improves at the cost of lower level of minimum remaining energy, that can lead to the risk of battery depletion during periods of energy scarcity. Therefore, the upper range of RE_{expect} (50%) is chosen which provides a good tradeoff of packet delay performance and minimum remaining energy level of the node. Furthermore, the threshold value, Eth is set to 10% and is applied to prevent complete battery depletion. During the investigation, different values of Eth (i.e., 15%, 20%, and 25%) have been incorporated and it has been observed that these values do not lead to significant impact on the performance.

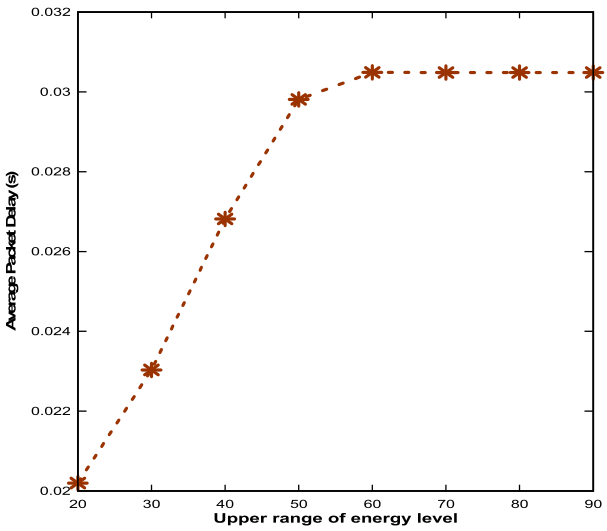

FIGURE 6. Average E2E delay of data packet for different upper ranges of RE_{expect}.

E. SELF-ADAPTATION TECHNIQUE

The receiver periodically wakes up to accept incoming packets from senders. On the other hand, sender nodes that hold data packets have to wait for WB to send their packets to the receiver. Due to this, they consume significant energy in listening to WB. Furthermore, they do not have the scheduling information of the receiver. Hence, these sender nodes have

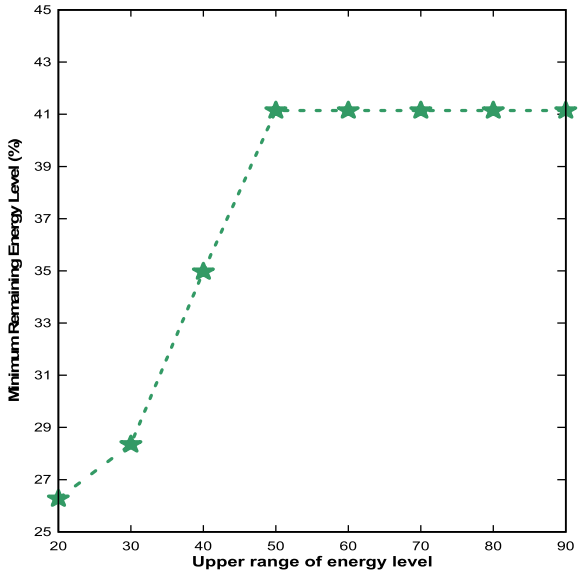

FIGURE 7. Minimum remaining energy level for different upper ranges of RE_{expect}.

to wait longer which leads to higher packet delays. To address these issues, the protocol uses a self-adaptation technique that assists in coordination between sender and receiver nodes. In this technique, the receiver shares its duty cycle through WB with all senders that provides the scheduling information of the receiver. Upon the reception of a WB, the sender node checks the d_c field and its buffer to determine if there is any data packet to send in the current cycle. If it holds a data packet, then it goes for CCA and transmits the packet. In case its buffer is empty, then it goes to sleep for the duration of T_{sleep}, which is computed using the d_c value received through WB. After that, it wakes up just before the receiver at the beginning of the next cycle. This approach helps sender nodes to coordinate with the receiver for successful data transmission, and also enables them to sleep, to conserve energy. The formula to compute T_{sleep} of the sender is as follows

$$T_{sleep} = (T_{listen} - (T_{WB} + T_{CCA}) + \frac{T_{listen} \times (1 - d_c)}{d_c}) \quad (8)$$

where T_{WB} denotes the transmission time of the WB beacon, and T_{CCA} represents channel sensing time.

The proposed self-adaptation technique allows the sender node to conserve energy by reducing idle listening. For example, consider a scenario where *Sender 1* (S_1) and *Sender 2* (S_2) receive WB from the receiver node that contains its duty cycle, as shown in Figure 8. After receiving WB, S_2 performs data transmission. However, since S_1 does not hold the data packet, thus, it goes to sleep following the receiver's wake-up schedule to conserve energy. Then, S_1 wake-up slightly before the receiver in the next cycle. It is essential to mention that if the receiver receives multiple Tx beacons with the same priority, i.e., P_1, then it chooses the sender node based on the first received Tx beacon.

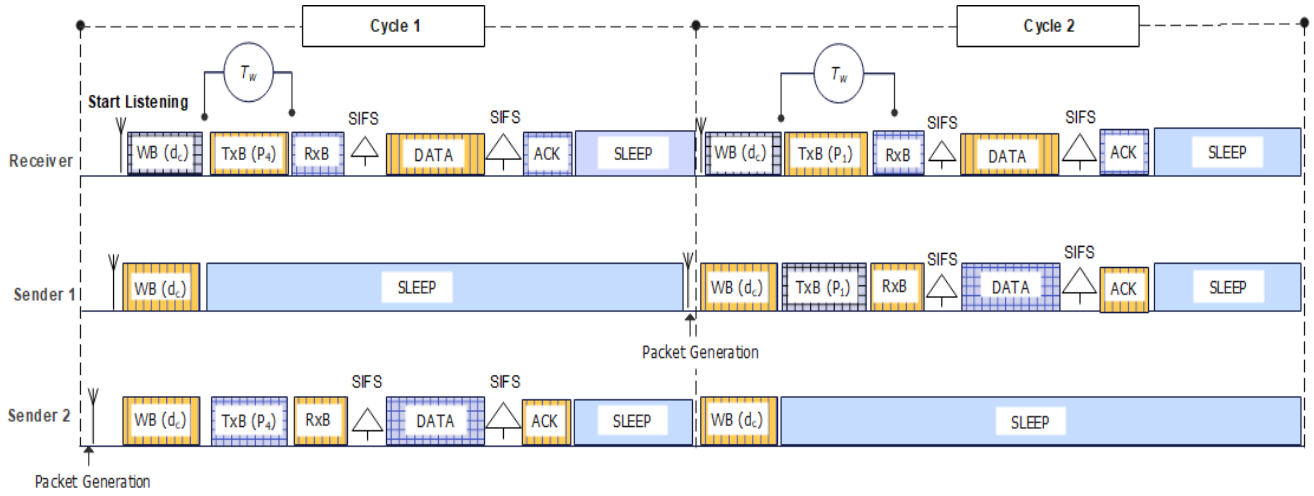

FIGURE 8. Data transmission using the self-adaptation technique.

IV. ENERGY MODEL AND PERFORMANCE METRICS

A. ENERGY MODEL

The energy model accounts for the total energy consumed and harvested by the node. The energy consumption, E_T of a node can be computed as follows

$$E_T = \sum_{i=0}^{n} P_i \times t_i \tag{9}$$

where p, t, and n denote the power consumption rate of radio state i, time spent in state i, and the number of states, respectively. For example, radio CC2420 [60] consumes power of 46.2 mW, 1.4 mW, 62 mW, and 62 mW in transmission, sleep, reception, and idle listening states, respectively. When the node turns ON its radio for transmitting or receiving a packet, the energy is deducted from the battery. The model also accounts for energy consumption when the node stays in the listening and sleep states.

The harvested energy, E_h of a node is computed using the following formula

$$E_h = \sum_{z=1}^{N} S \times P_s \times P_e \times d_s \tag{10}$$

where z and S represent the number of simulation hours and realistic solar irradiance (W/m^2) obtained from NREL [61], respectively.

B. PERFORMANCE METRICS

1) END-TO-END DELAY

The E2E delay refers to the total time between the generation of the packet at the source and until its reception at the destination. It can be calculated as follows

$$E2Edelay = D_{queu} + D_{trans} + D_{prop} + D_{proc} \tag{11}$$

where D_{proc}, D_{queu}, D_{prop}, and D_{trans} represent processing, queuing, propagation, and transmission delays, respectively.

2) PACKET DELIVERY RATIO

It is the ratio of the total number of packets received (NP_{PktR}) by the receiver to the total number of packets sent by the senders (NP_{PktT}). It is computed in percentage as follows

$$PDR = \frac{NP_{PktR}}{NP_{PktT}} \times 100 \tag{12}$$

3) NETWORK THROUGHPUT

The average network throughput (N_{Th}) refers to the amount of data packets received by the receiver over the total simulation time (T_s), as given below

$$N_{Th} = \frac{NP_{PktR} \times L_{Pkt}}{T_s} \tag{13}$$

where L_{Pkt} represents the size of the data packet in bits.

4) AVERAGE ENERGY CONSUMPTION PER BIT

The average energy consumption per bit (E) can be computed by dividing the total energy consumption with total number of data packet bits received, as given below

$$E = \frac{E_T}{NP_{PktR} \times L_{Pkt}} \tag{14}$$

and E_T can be calculated using Eq. (9).

5) TOTAL ENERGY CONSUMPTION

The total energy consumption, E_{total} is the sum of energy consumed by the receiver and sender nodes. It can be computed as follows

$$E_{total} = E_{TR} + (N_s \times E_{TS}) \tag{15}$$

where E_{TR} and E_{TS} denotes the energy consumption of the receiver and sender nodes, respectively. E_{TR} and E_{TS} can be computed using Eq. (9).

V. RESULTS AND DISCUSSION

To evaluate the protocol's performance, we have implemented the proposed MAC protocol in GreenCastalia [62], an extension of the Castalia 3.3 simulator [63]. Castalia is an open-source network simulator and is built with OMNeT++ [64]. It is a widely used and actively maintained network simulator in the WSN research community. In GreenCastalia, the implementation of a sensor node follows a modular approach, and each module is connected through connections. Furthermore, it enables the development and simulation of EH protocols and algorithms using different energy harvesters and rechargeable storages. For instance, it allows the user to define the EH source, such as a solar cell to harvest energy with particular efficiency. In addition, parameters such as solar panel size and efficiency can be defined. Similarly, the user can choose a suitable storage device i.e. rechargeable battery to store the energy and is allowed to set parameters such as maximum capacity, and initial battery capacity as per the application's requirement. In this work, a rechargeable battery is implemented with a solar cell as the EH device. Moreover, it supports realistic radio modules and wireless channels. For example, the user can define the radio model, i.e., CC2420 [60], and add a new MAC or modify existing protocols. The performance of PADC-MAC is evaluated under different harvesting scenarios. Furthermore, to demonstrate the PADC-MAC performance, real-life solar data is utilized for four consecutive days (96 hours of simulations) from August 9-13, 2011 (high irradiance) and October 24-27, 2011 (low irradiance), which includes high and low EH scenarios. The parameters such as operating voltage, and power consumption of radio states are taken from the widely used TelosB node and Texas Instruments CC2420 wireless transceiver, respectively [65], [66]. The receiver is connected with a commercial IXOLAR solar panel [67] of 7.7 cm^2 in size and with an efficiency of 22%. In addition, it employs a rechargeable battery with a maximum capacity of 1500 mAh i.e. 12960 J. Moreover, it is optimized for the network that has a smaller number of sending nodes per receiver. For instance, a large size sensor network can be divided into several smaller-sized networks, called clusters to achieve benefits like optimizing energy efficiency, and scalability [68]. Therefore, its performance is evaluated using a single-hop scenario and network topology consists of a receiver and 7 sender nodes which are located within an area of 30 m $\times$ 30 m, as shown in Figure 9. A similar network topology was also considered in [69]. Each sender node generates 345600 packets with a rate of 1 packet per second with a size of 33 bytes and transmits to the receiver using the p-persistent CSMA approach, where the p-value is set as $1/N_s$, where N_s represents the number of sender nodes. The reason behind choosing the p-persistent CSMA is that it takes a moderate and balanced approach between 1-persistent and non-persistent CSMA [70]. Moreover, in asynchronous protocols, it helps to reduce packet collision and improve efficiency [71]. Furthermore, it has been widely considered in the literature for designing MAC protocols [34], [71], [72], [73], [74]. For a fair comparison, all protocols follow the same p-persistent CSMA approach for Tx beacon transmissions. Other CSMA schemes such as 1-persistent and nonpersistent CSMA as may lead to a higher chance of collision and reduce the network efficiency [75]. WSN nodes support a small size of data packets, thus, the packet size of 33 bytes is chosen which is also commonly used in the literature [76], [77], [78]. The size of beacons is chosen in conformance to the IEEE 802.15.4 standards, while also considering the specific fields defined for each beacon. The MAC buffer and physical frame overheads are set to 32 packets, and 6 bytes, respectively [79]. The duration of T_w is set to accommodate the time required for all sender nodes to send their Tx beacons successfully to the receiver. Likewise, T_{listen} provides sufficient time for the receiver to stay active in the current cycle to receive the packet from the selected sender. The performance of the PADC-MAC is evaluated in terms of average E2E delay for the highest priority packet and all packets, PDR, network throughput, energy consumption per bit, receiver energy consumption, and total network energy consumption in the network. For performance comparison, three well-known MAC protocols for EH-WSNS, namely QPPD-MAC, QAEE-MAC, and EEM-MAC are also implemented. Table 4 shows the simulation parameters.

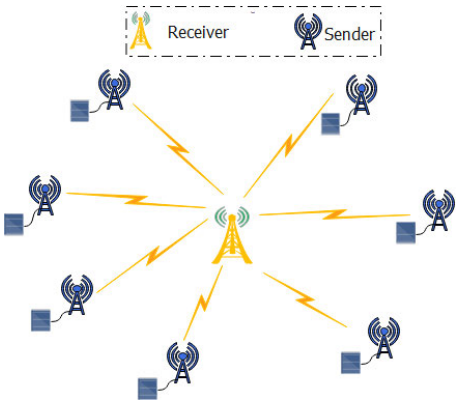

FIGURE 9. Network topology used in performance evaluation.

Firstly, we present the performance evaluation of the proposed NARNET model and its comparisons with EWMA and actual data under dynamic harvesting conditions. Secondly, the performance evaluation of the proposed PADC-MAC protocol, which incorporates energy prediction results obtained using NARNET in the GreenCastalia simulator under high and low solar irradiance scenarios, is presented. Finally, simulation results in average E2E delay for the highest priority packet and all packages, PDR, network throughput, energy consumption per bit, receiver energy consumption, and total network energy consumption are discussed and compared with QPPD-MAC, QAEE-MAC, and EEM-MAC protocols. It has been noted that PDR, and network throughput results are the same in all protocols. Therefore, only results for high solar irradiance are shown.

TABLE 4. Simulation parameters.

Parameter	Value
Simulation time	96 hours
Data packet	33 bytes
Tx beacon	14 bytes
ACK packet	11 bytes
Rx beacon	13 bytes
Wake-up beacon	13 bytes
Physical frame overhead	6 bytes
Solar panel size	7.7 cm^2
Harvesting rate	Variable
Panel efficiency	22%
Retransmission limit	10
Maximum buffer limit	32
Sender nodes	1 to 7
Area	30 m × 30 m
Sensor node	Telos Rev B
Operating voltage	2.4 V
Data rate	250 kbps
CCA check delay	0.128 ms
SIFS	0.192 ms
T_{listen}	17 ms
T_w	5 ms
Slot size	320 µs
Transmission power	46.2 mW
Reception power	62 mW
Idle listening power	62 mW
Sleep power	1.4 mW
E_{max}	12960 J
E_{th}	10%
Initial battery level	45%

A. PERFORMANCE EVALUATION OF THE NARNET MODEL

The NARNET model is implemented in MATLAB R2022a to predict the hourly solar irradiance value. Thus, each day is divided into 24 timeslots. The developed model has one-dimensional solar irradiance data measured by NREL [61]. The data contains 13862 samples of solar irradiance for 19 months from April 1, 2010, to October 31, 2011, incorporating seasonal variations. The model is trained offline using available NREL data from April 2010 to June 2011 and tested using the data from July 2011 to October 2011, which includes dynamic solar irradiance scenarios. Furthermore, the performance has been compared with EWMA using different months' data, i.e., August (high harvesting) and October (low harvesting) scenarios. The prediction error is computed using the Mean Absolute Error (MAE)

$$MAE\ (\%) = \frac{\sum \left| S_t - \check{S}_t \right|}{\sum S_t} \times 100 \tag{16}$$

where S_t and $\check{S}_t$ are actual and predicted irradiance during timeslot t, respectively.

Figure 10 and Figure 11 show high solar irradiance and corresponding energy obtained using the solar panel, respectively. The results compare the prediction performance of the proposed NARNET with actual data and EWMA for four consecutive days, i.e., 9th to 13th August 2011. For a fair comparison, the weighting factor (α) in EWMA is set to 0.5, which provides the lowest error [80]. The results show that the proposed model closely follows the actual trend and accurately predicts the incoming irradiance with a correlation coefficient (R) of 0.98 and MAE of 11.75%. In contrast, EWMA achieves R of 0.96 and provides the MAE of 16.90%, which is 30.47% more compared to NARNET. This is because it incorporates energy intake at the same time as on previous days to perform the prediction for the next slot. As a result, it fails to adapt to sudden changes in

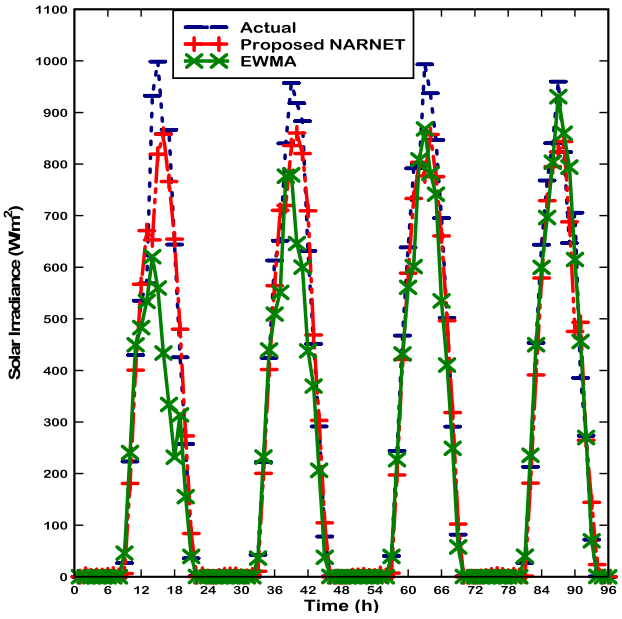

FIGURE 10. Average hourly solar irradiance for four consecutive days, 9th to 13th August 2011, versus simulation time.

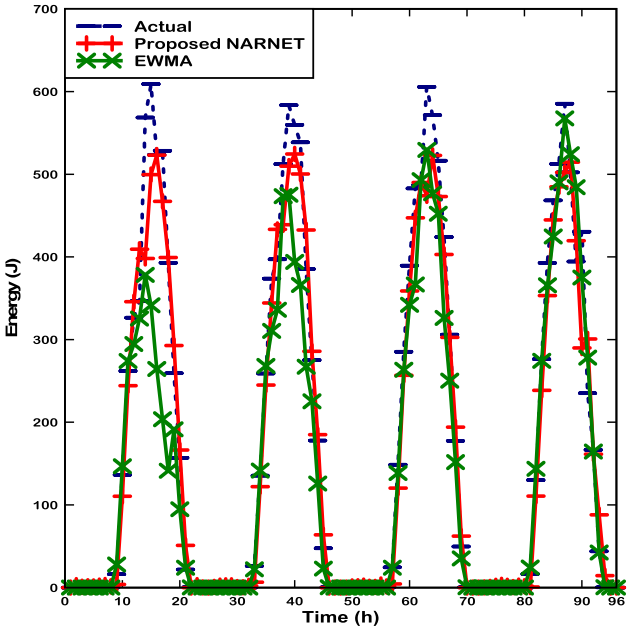

FIGURE 11. Comparison of predicted energy obtained using NARNET and EWMA with actual energy for four days consecutive days, 9th to 13th August 2011.

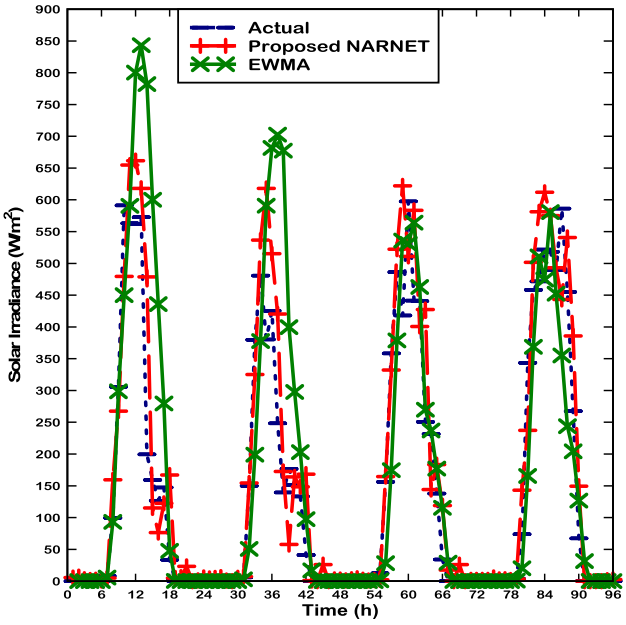

FIGURE 12. Average hourly solar irradiance for four consecutive days, 24th to 27th October 2011, versus simulation time.

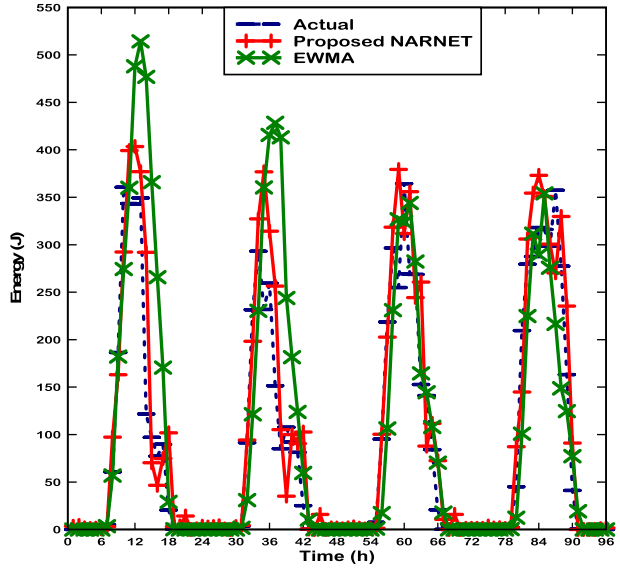

FIGURE 13. Comparison of predicted energy obtained using NARNET and EWMA with actual energy for four days consecutive days, 24th to 27th October 2011.

weather conditions, particularly on the first day, which leads to higher *MAE*.

Figure 12 and Figure 13 present low solar irradiance data and corresponding energy for four consecutive days, i.e., 24th to 27th October 2011. The results show that the NARNET attains good agreement with the actual energy and provides *R* and *MAE* of 0.95 and 28.46%, respectively, which are marginally different than Figure 10. This is because weather conditions are changing consistently every day. On the other hand, sudden weather changes also degrade EWMA performance. It achieves an *R* of 0.82 and provides *MAE* of 39.48%, respectively, which is 28% more than NARNET.

B. PERFORMANCE EVALUATION OF PADC-MAC PROTOCOL UNDER HIGH SOLAR IRRADIANCE

The receiver remaining energy, RE_{total} in all protocols is given in Figure 14. The initial battery level is set to 45%, and the day starts at midnight. It declines as solar energy is unavailable until sunrise (shown in the high solar irradiance scenario Figure 10), and the receiver incorporates its stored energy to carry out communication tasks. After sunrise, its values gradually increase to 62.5%, 65.7%, 65.8%, and 66.1% in PADC-MAC, QPPD-MAC, QAEE-MAC, and EEM-MAC, respectively, on the first day. Then, it declines again as harvesting energy is unavailable after sunset. During the last three days, sufficient harvesting energy was available. Thus, its values reach 98.7%, 98.8%, 99.3%, and 98.8% at the end of the fourth day. It can be noticed that PADC-MAC has a lower RE_{total} values during 18h to 90h when compared to other protocols. This is because of two reasons. First, it regulates the receiver duty cycle using available energy and performs more aggressively to shorten the delay, resulting in a decrease in RE_{total}. Furthermore, it incorporates knowledge of future energy intake (given in Figure 11) to optimize the network performance further. Thus, it increases its duty cycle to 1 when sufficient energy is available in the next hour and is more than the required energy, E_c. However, other protocols do not consider energy prediction and do not perform aggressively even though adequate energy is available during the daytime for all days.

Figure 15 presents the duty cycle of the receiver. Initially, PADC-MAC, QPPD-MAC, and QAEE-MAC start their operation with a duty cycle value of 50%, while its value is set to 56% in EEM-MAC. Subsequently, the duty cycle decreases to 45.4%, 45.5%, and 54.3% in PADC-MAC, QPPD-MAC, and EEM-MAC, respectively. The reason is that in these protocols, the receiver incorporates RE_{total} to adjust its duty cycle values, which decline as solar energy is unavailable until sunrise. In PADC-MAC, the duty cycle rises to 1 for the following three days. Its battery is sufficiently charged to more than 50% for the following days, and the duty cycle is increased to reduce sleep time. This helps the receiver to stay active most of the time for almost 86 hours and to minimize delay for the incoming packets. In addition, it also incorporates predicted harvesting energy in the next hour, i.e., $HE_{predicted}$ and uses this information in duty cycle adjustment to further improve performance. In contrast, in QPPD-MAC, QAEE-MAC, and EEM-MAC, the receiver becomes more conservative despite adequate energy resources for all consecutive days; thus, they have missed the opportunity to improve their performance.

Figure 16 shows the average E2E delay for different priority packets. The result indicates that PADC-MAC provides a meaningful reduction in delay for P_4 packets of up to 13.5%, 46%, and 28% compared to QPPD-MAC, QAEE-MAC, and EEM-MAC, respectively, across all sender nodes. The reason is that both PADC-MAC and QPPD-MAC support the P_4 priority packets by canceling the T_w when they arrive. Furthermore, PADC-MAC utilizes the harvested energy to

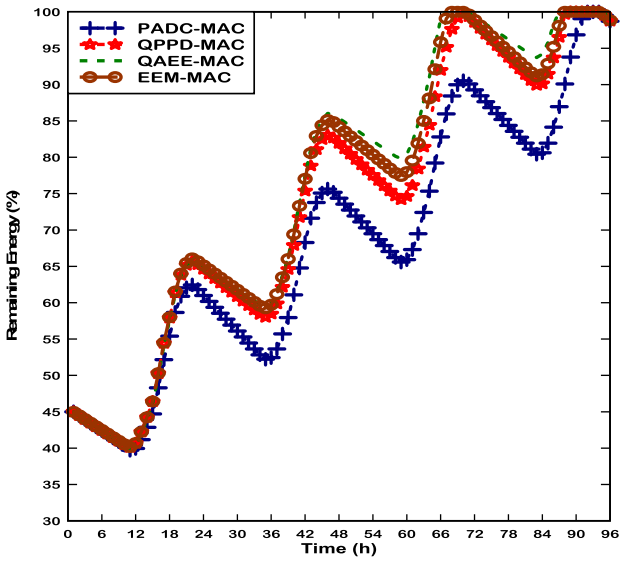

FIGURE 14. Remaining energy of the receiver.

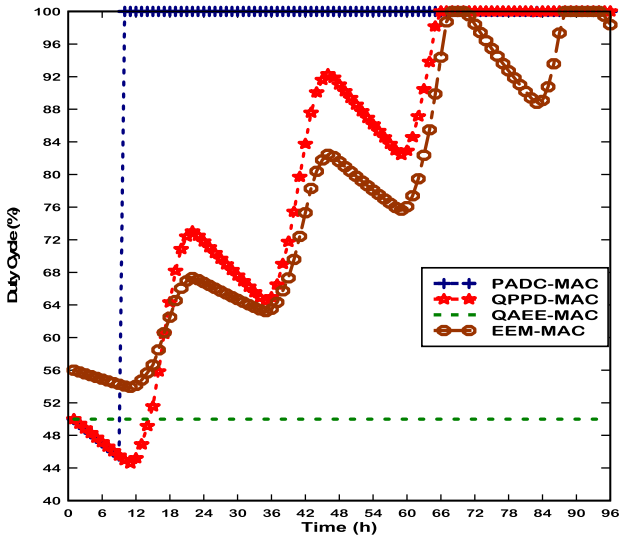

FIGURE 15. Duty cycle of the receiver.

increase the duty cycle aggressively when possible, by maximizing its duty cycle corresponding to its residual energy level and the potential increase in energy level in the near future. Therefore, considering battery capacity and incoming harvested energy, the receiver operates on the maximum duty cycle, i.e., 1. As a result, the radio remains active most of the time, which decreases the delay for incoming priority packets, P_4. In contrast, QPPD-MAC, QAEE-MAC, and EEM-MAC are more energy-conservative and operate without incorporating incoming harvested energy. Thus, the data packets suffer long delays despite sufficient energy resources. It can be seen that QAEE-MAC has the highest average delay for priority packets than other protocols. This is because it operates on a fixed duty cycle and does not consider current harvesting to enhance performance.

The average E2E delay of all packets is given in Figure 17. Again, PADC-MAC outperforms the other three protocols. Furthermore, the result shows that PADC-MAC provides the

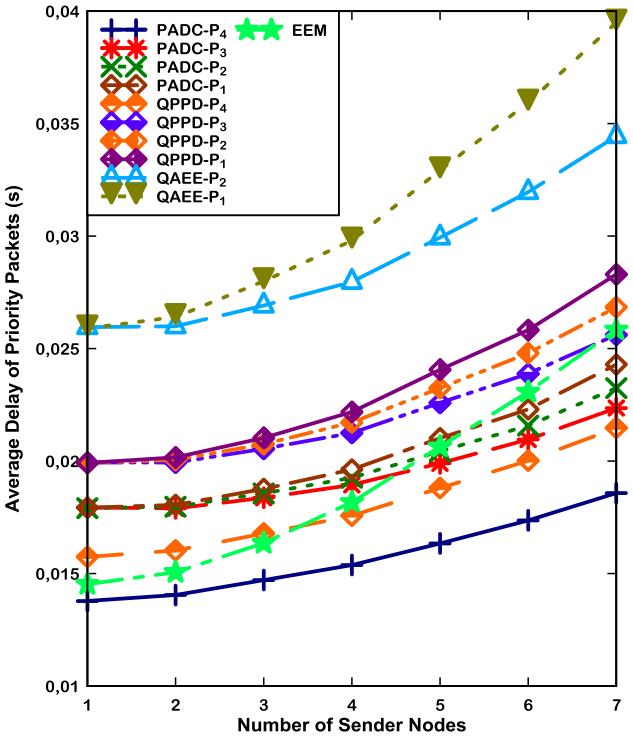

FIGURE 16. Average E2E delay for priority packets.

lowest packet delay by up to 13.5%, 40.2%, and 14.4% compared to QPPD-MAC, QAEE-MAC, and EEM-MAC, respectively. The reason is that it increases the duty cycle based on the remaining energy level and the potential increase in energy in the near future. The result also indicates that EEM-MAC performs slightly better than PADC-MAC when the number of sender nodes is 1–4. First, it allows nodes to transmit their packets without any priority. Second, a few sender nodes experience low contention in accessing the medium and, as a result, lower average delay. However, EEM-MAC performance decreases compared to PADC-MAC when the number of sending nodes is 5-7. The reason is that when there are a higher number of sender nodes, nodes try to access the medium simultaneously without priority differentiation, which increases packet delay.

PDR of all protocols is presented in Figure 18. It can be noticed that all protocols achieve almost 100% PDR across all numbers of sensor nodes. This is because the receiver in all protocols has sufficient energy to maintain its operation and is available to collect the incoming packets. The average network throughput performance of all protocols is shown in Figure 19. It increases linearly with the number of sender nodes. The result indicates the maximum value of 1568 bps when the number of sending nodes is 7.

The energy consumption per bit is given in Figure 20. It increases linearly because more packets are transmitted in the network at a higher number of senders. In PADC-MAC, it decreases significantly by up to 81% in comparison to the other three protocols. This is because the PADC-MAC uses self-adaptation in which the receiver shares its following

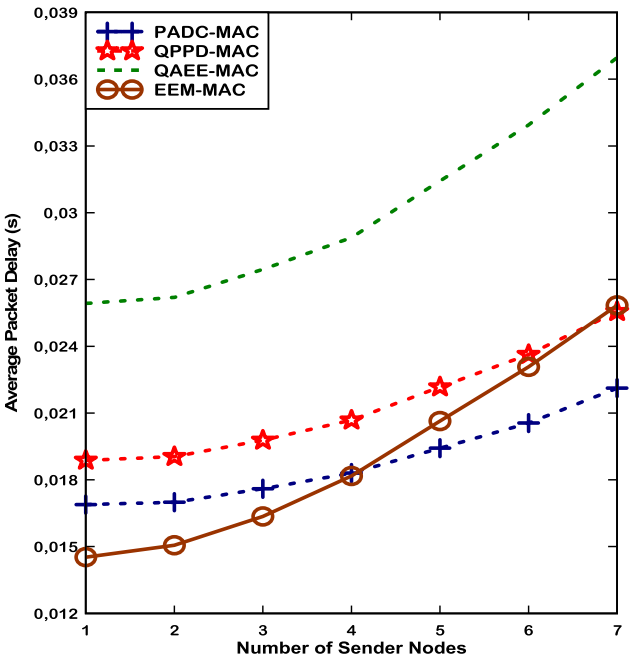

FIGURE 17. Average E2E delay of all packets.

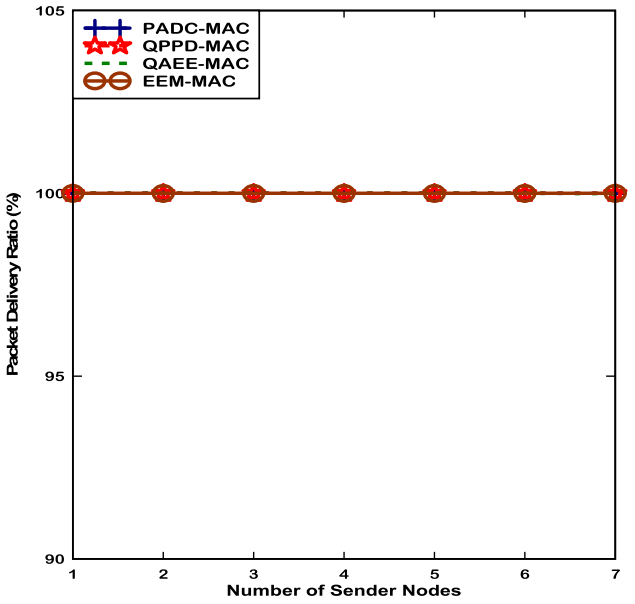

FIGURE 18. Packet delivery ratio.

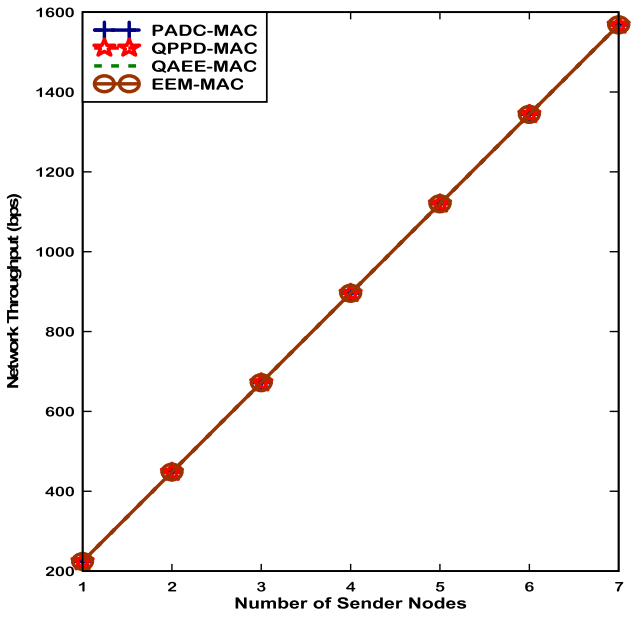

FIGURE 19. Network throughput.

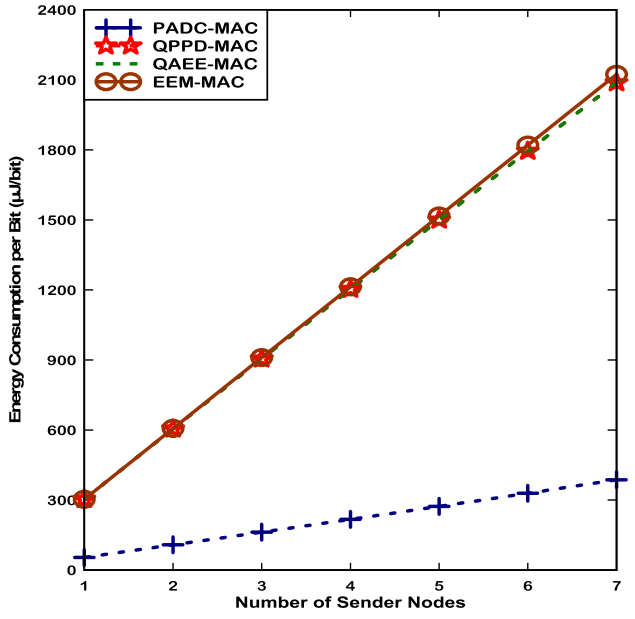

FIGURE 20. Energy consumption per bit.

wake-up schedule with all sender nodes through the WB. After receiving the WB, the sender nodes that have data packets contend for the medium to perform data transmission. Other sender nodes incorporate the receiver's wake-up schedule and adjust their sleep time to wake up just before the receiver. As a result, nodes conserve energy by reducing idle listening. In other protocols, sender nodes are usually active, which leads to an increase in energy consumption. It can also be seen that both QPPD-MAC and QAEE-MAC have a slightly lower values compared to EEM-MAC. The reason is that these protocols use the RX beacon that contains a NAV value. After RX-beacon, the non-selected sender nodes sleep until the NAV timer expires, which conserves energy.

The receiver energy consumption (E_r) is given in Figure 21. The PADC-MAC spends more energy by up to 14.7%, 50.4%, and 26% compared to QPPD-MAC, QAEE-MAC, and EEM-MAC, as expected. This is because the receiver in PADC-MAC becomes more aggressive when it has sufficient energy available and aims to use it efficiently to optimize the network performance. Thus, it increases the duty cycle by shortening sleep time. Moreover, it also incorporates expected harvesting energy in the next hour to increase the duty cycle further. This helps reduce packet delay at the cost of a slight energy consumption increase when sufficient harvesting energy is available.

In other protocols, the receiver becomes more energy-conservative, resulting in lower energy consumption than

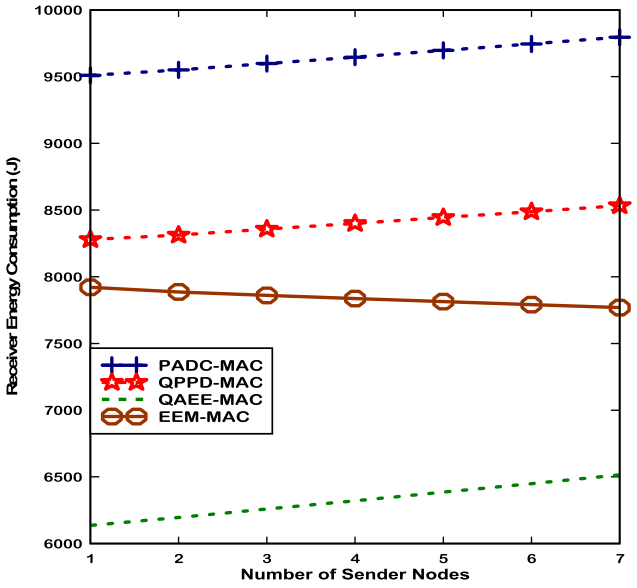

FIGURE 21. Receiver energy consumption.

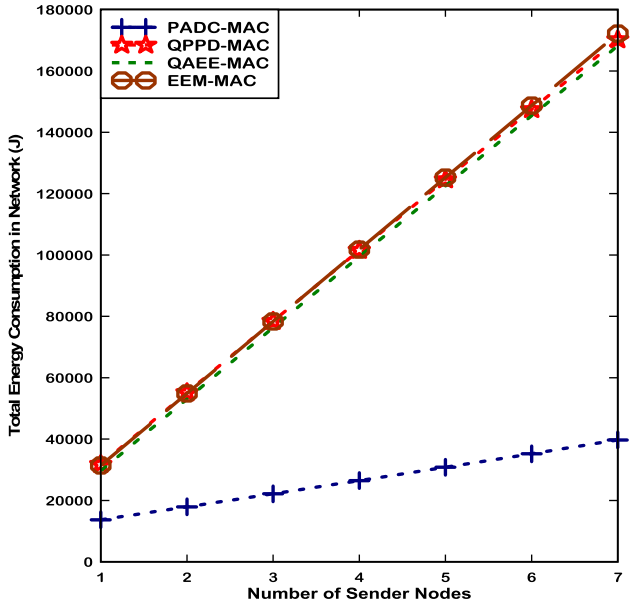

FIGURE 22. Total energy consumption.

PADC-MAC. However, it can also be seen that the energy consumption slightly increases with the varying number of nodes. This is because the receiver accepts more packets. In addition, the receiver has to wait until it gets the highest priority packet. On the other hand, energy consumption slightly decreases in EEM-MAC for the higher number of sending nodes. The reason is that EEM-MAC does not employ Tx beacon and Rx beacon, and the receiver does not wait for a specific packet. Thus, after receiving the first data, it sleeps to conserve energy.

Figure 22 shows the total energy consumption. It combines the receiver's energy consumption and the sender nodes' total energy consumption. It can be noticed that the PADC-MAC shows a significant reduction of up to 76.6%, 76.4%, and 76.9% in the total energy consumption when compared to QPPD-MAC QAEE-MAC, and EEM-MAC, respectively. This is because the PADC-MAC uses a novel self-adaptation technique that helps sender nodes to conserve energy. This leads to reducing overall energy consumption. In contrast, QAEE-MAC provides a marginally lower value compared to QPPD-MAC and EEM-MAC. Because in QAEE-MAC, the receiver energy consumption is lower than QPPD-MAC and EEM-MAC, resulting in slightly lower total energy consumption.

C. PERFORMANCE EVALUATION OF PADC-MAC PROTOCOL UNDER LOW SOLAR IRRADIANCE SCENARIO

The remaining energy is presented in Figure 23. Initially, it declines as sunlight is unavailable until morning (as shown in the low solar irradiance scenario, Figure 12). Then, it increases until noon and reaches 46.7%, 48.8%, 48.8%, and 49.2% in PADC-MAC, QPPD-MAC, QAEE-MAC, and EEM-MAC, respectively. It follows a similar trend for the next three days. It can be noticed that its value is significantly lower than those in the high irradiance scenario. Moreover, the battery remains charged up to 49.4%, 58.9%, 60.7%, and 61.1% in PADC-MAC, QPPD-MAC, QAEE-MAC, and EEM-MAC, respectively, at the end of the last day. It can be seen that PADC-MAC has a lower value in comparison to other protocols. This is because the PADC-MAC becomes more aggressive when sufficient energy is available. Thus, it increases the duty cycle by considering both remaining and forecasting energy values to decrease the packet delay. As a result, the remaining energy is decreased.

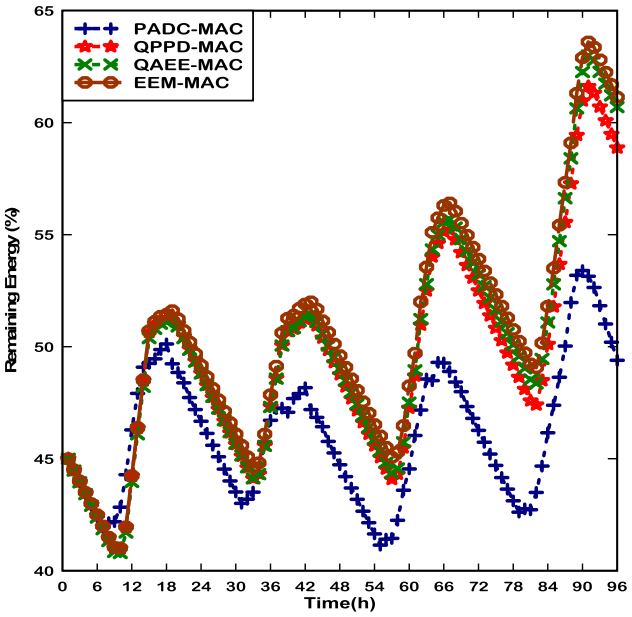

FIGURE 23. Remaining energy of the receiver.

The duty cycle, d_c of the receiver is given in Figure 24. The result shows significant variation in PADC-MAC compared to other protocols. In addition, its value changes abruptly to maximum, i.e., 1 in certain hours, mainly during the daytime, almost seven times. Then, it returns suddenly and follows

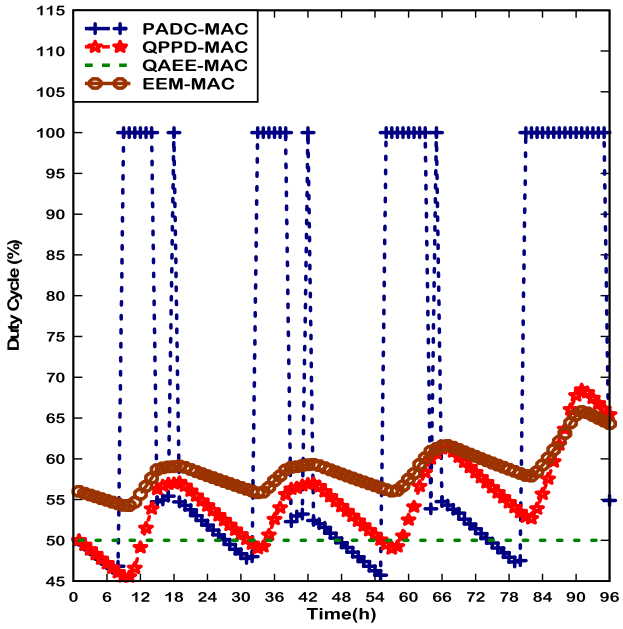

FIGURE 24. Duty cycle of the receiver.

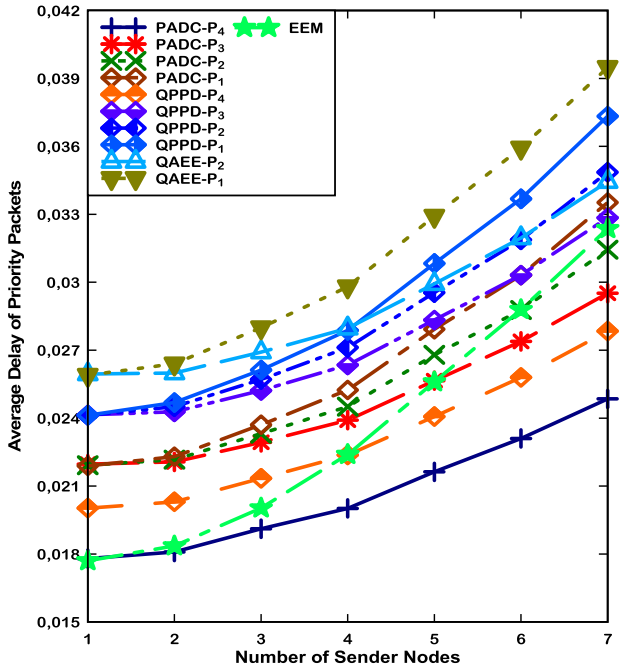

FIGURE 25. Average E2E delay for priority packets.

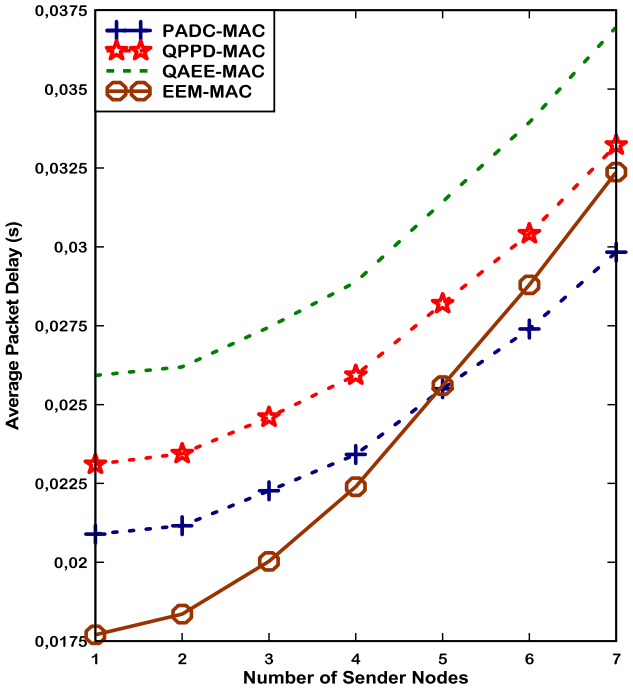

FIGURE 26. Average E2E delay of all packets.

a continuous trend as QPPD-MAC and EEM-MAC. This is because it incorporates the remaining energy and predicted energy value as given in Figure 23 and Figure 13, respectively, to adjust the receiver duty cycle. During certain hours of the day, it meets the condition that the expected energy value is greater than the maximum required energy in an hour. This leads to increasing the duty cycle to a maximum value, i.e., 1, to enhance the network performance. Moreover, small changes in the duty cycle are due to weather conditions such as cloud cover that could suddenly appear and disappear. On the other hand, QAEE-MAC uses a fixed duty cycle, i.e., 0.5, and thus shows a straight line.

Figure 25 shows the average E2E delay for priority packets. In PADC-MAC, the highest priority packet, P_4 experiences less delay by up to 10.7%, 27.8%, and 23.2% compared to P_4 in QPPD-MAC, P_2 in QAEE-MAC, and the average of all packages in EEM-MAC. This is due to the duty cycle adjustment mechanism, which allows the PADC-MAC's receiver to increase its duty cycle when sufficient energy resources are available. Thus, it wakes up frequently to collect the priority packets. As a result, it minimizes the waiting time for priority packets to reduce the delay. Nevertheless, it can be seen that PADC-MAC suffers slightly higher delays for other priority packets when compared to the highest priority packet of QPPD-MAC. This is because it aims to meet the requirement of transmitting the highest priority packet, P_4, faster than others priority packets. Thus, lower priority packets experience longer delays before their transmission. It can also be seen that delay in all protocols increases linearly with a different number of sender nodes. The reason is that more nodes contend for the medium, contributing to a higher average delay.

The average E2E delay for all packets is given in Figure 26. The result shows that the PADC-MAC outperforms other protocols when the number of sender nodes is 5-7. Furthermore, the PADC-MAC offers a meaningful reduction of up to 10.2%, 19.3%, and 7.8% compared to QPPD-MAC, QAEE-MAC, and EEM-MAC, respectively. The reason is that the receiver follows the duty cycle adjustment mechanism, which allows the receiver to increase its listening time while considering its current energy level and incoming harvested energy to reduce delay. It can also be noticed that EEM-MAC provides better performance than QPPD-MAC and QAEE-MAC. This is because the receiver of EEM-MAC

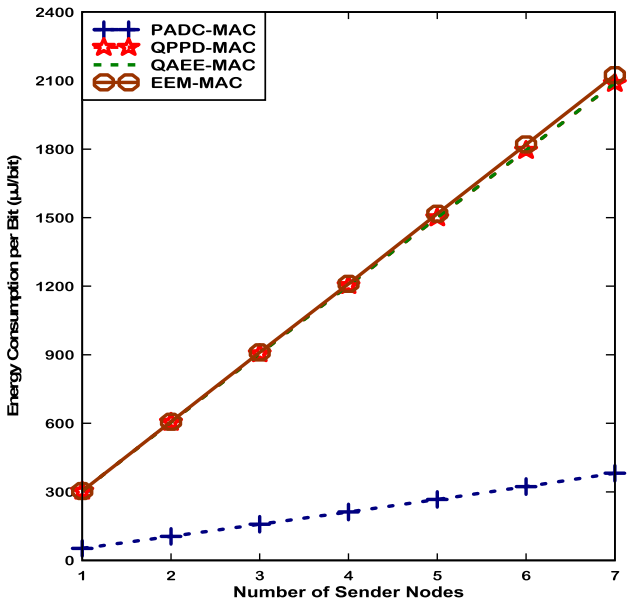

FIGURE 27. Energy consumption per bit.

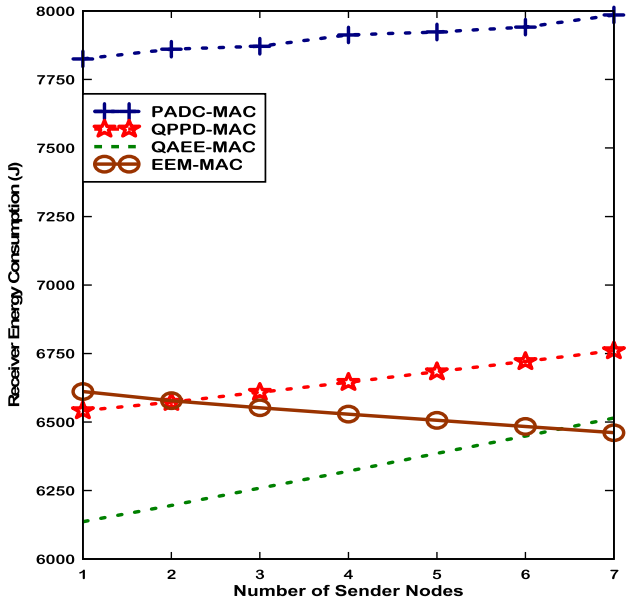

FIGURE 28. Receiver energy consumption.

has a higher duty cycle than both protocols, resulting in a lower average packet delay.

Figure 27 presents the energy consumption per bit in all three protocols. PADC-MAC achieves better performance by up to 81.7% compared to QPPD-MAC and QAEE-MAC and up to 82% compared to EEM-MAC. The reason is that it uses a self-adaptation technique that enables senders to adjust the wake-up schedule accordingly so that they can wake up slightly before the receiver to conserve energy. In other protocols, the sender nodes are usually active, which increases energy consumption. It can be noticed that PADC-MAC has almost the same performance in both scenarios because the same number of packets are delivered in the networks. Moreover, QPPD-MAC and QAEE-MAC provide slightly

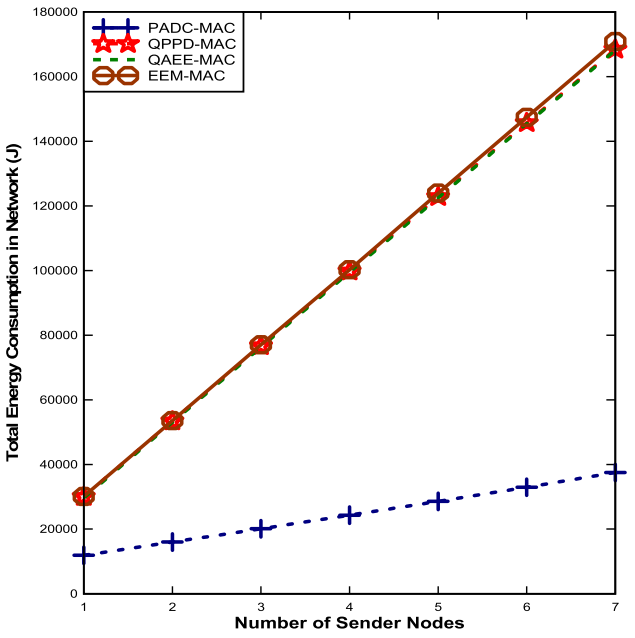

FIGURE 29. Total energy consumption.

lower values compared to EEM-MAC. This is because both protocols use RX beacon that contains NAV value. After receiving RX-beacon, the non-selected sender nodes sleep until the NAV timer expires, which conserves energy.

Figure 28 presents the energy consumption of the receiver in all protocols. The PADC-MAC has higher energy consumption by up to 18.1%, 22.6%, and 23.6% compared to QPPD-MAC, QAEEM-MAC, and EEM-MAC, respectively, as expected. The reason is that PADC-MAC aims to optimize network performance when sufficient energy is available. Thus, it increases its duty cycle more aggressively to decrease the packet delay. As a result, it consumes higher energy. However, other protocols become more conservative even though sufficient resources are available. As a result, packets suffer longer delays.

The total energy consumption in the network is given in Figure 29. It can be seen that the PADC-MAC reduces energy consumption by up to 77.7%, 77.7%, and 78% compared to QPPD-MAC, QAEE-MAC, and EEM-MAC, respectively. This is because the self-adaptation technique allows the sender to conserve energy, resulting in, overall energy consumption decreases in the network.

VI. CONCLUSION AND FUTURE WORK

EH technology is a promising solution to power up sensors using energy sources from the ambient environment. However, dynamic weather conditions leads to uncertainty in harvesting rates. This drives the development of EH adaptive MAC protocols. In this paper, a novel and more realistic prediction-based adaptive duty cycle MAC protocol has been developed for EH-WSNs, called PADC-MAC. Furthermore, PADC-MAC incorporates the future harvested energy obtained from NARNET ML model to plan the available energy using a duty cycle adjustment scheme. As a result,

the receiver sets its duty cycle based on the predicted incoming harvested energy to enhance network performance. Furthermore, it supports QoS through traffic differentiation and enables the receiver node to perform more aggressively when it has a sufficient inflow of incoming harvested energy to decrease the packet delay for P_4 in the network. In addition, the self-adaptation technique has been introduced to mitigate the idle listening of contending senders and preserve energy in the network.

The performance of PADC-MAC has been evaluated in terms of average E2E delay for priority and all packets, PDR, network throughput, energy consumption per bit, receiver energy consumption, and total network energy consumption using high and low solar irradiance data. The simulations have been performed for 96 consecutive hours using GreenCastalia and compared with three state-of-the-art receiver-initiated MAC protocols. In both scenarios, the PADC-MAC demonstrates a significant reduction in average E2E delay of the highest priority packets and all packets, energy consumption per bit, and total energy consumption of more than 10.7%, 7.8%, 81%, and 76.4% when compared to QPPD-MAC, QAEE-MAC, and EEM-MAC protocols. The future research works will include extending the PADC-MAC to support multi-hop for applications in large scale EH-WSNs. In addition, validating the PADC-MAC protocol using hardware testbeds for the specific application that generates different data packets in the network, can also be undertaken.

REFERENCES

[1] S. Bebortta, D. Senapati, and N. Rajput, "Evidence of power-law behavior in cognitive IoT applications," *Neural Comput. Appl.*, vol. 32, pp. 16043–16055, May 2020.

[2] T. Ruan, Z. J. Chew, and M. Zhu, "Energy-aware approaches for energy harvesting powered wireless sensor nodes," *IEEE Sensors J.*, vol. 17, no. 7, pp. 2165–2173, Apr. 2017.

[3] R. Mukherjee, A. Kundu, I. Mukherjee, D. Gupta, P. Tiwari, A. Khanna, and M. Shorfuzzaman, "IoT-cloud based healthcare model for COVID-19 detection: An enhanced *k*-nearest neighbour classifier based approach," *Computing*, pp. 1–21, Apr. 2021.

[4] H. Magsi, A. H. Sodhro, M. S. Al-Rakhami, N. Zahid, S. Pirbhulal, and L. Wang, "A novel adaptive battery-aware algorithm for data transmission in IoT-based healthcare applications," *Electronics*, vol. 10, no. 4, pp. 1–17, 2021.

[5] A. H. Sodhro, Y. Li, and M. A. Shah, "Energy-efficient adaptive transmission power control for wireless body area networks," *IET Commun.*, vol. 10, no. 1, pp. 81–90, 2016.

[6] M. M. Sandhu, S. Khalifa, R. Jurdak, and M. Portmann, "Task scheduling for energy-harvesting-based IoT: A survey and critical analysis," *IEEE Internet Things J.*, vol. 8, no. 18, pp. 13825–13848, Sep. 2021.

[7] S. Kosunalp, "A new energy prediction algorithm for energy-harvesting wireless sensor networks with *Q*-learning," *IEEE Access*, vol. 4, pp. 5755–5763, 2016.

[8] H. Sharma, A. Haque, and Z. A. Jaffery, "Solar energy harvesting wireless sensor network nodes: A survey," *J. Renew. Sustain. Energy*, vol. 10, no. 2, pp. 1–33, 2018.

[9] A. Jushi, A. Pegatoquet, and T. N. Le, "Wind energy harvesting for autonomous wireless sensor networks," in *Proc. Euromicro Conf. Digit. Syst. Design (DSD)*, Limassol, Cyprus, Aug. 2016, pp. 301–308.

[10] C. Covaci and A. Gontean, "Piezoelectric energy harvesting solutions: A review," *Sensors*, vol. 20, no. 12, pp. 1–37, 2020.

[11] G. Famitafreshi, M. S. Afaqui, and J. Melià-Segui, "A comprehensive review on energy harvesting integration in IoT systems from MAC layer perspective: Challenges and opportunities," *Sensors*, vol. 21, no. 9, pp. 1–53, 2021.

[12] N. S. Hudak and G. G. Amatucci, "Small-scale energy harvesting through thermoelectric, vibration, and radiofrequency power conversion," *J. Appl. Phys.*, vol. 103, no. 10, pp. 1–5, 2008.

[13] D. P. Kumar, A. Tarachand, and C. S. R. Annavarapu, "Machine learning algorithms for wireless sensor networks: A survey," *Inf. Fusion*, vol. 49, pp. 1–25, Sep. 2019.

[14] M. A. Alsheikh, S. Lin, D. Niyato, and H. P. Tan, "Machine learning in wireless sensor networks: Algorithms, strategies, and applications," *IEEE Commun. Surveys Tuts.*, vol. 16, no. 4, pp. 1996–2018, 4th Quart., 2014.

[15] A. Sharma and A. Kakkar, "A review on solar forecasting and power management approaches for energy-harvesting wireless sensor networks," *Int. J. Commun. Syst.*, vol. 33, no. 8, pp. 1–33, 2020.

[16] H. Sharma, A. Haque, and F. Blaabjerg, "Machine learning in wireless sensor networks for smart cities: A survey," *Electronics*, vol. 10, no. 9, pp. 1–22, 2021.

[17] A. Sharma and A. Kakkar, "Forecasting daily global solar irradiance generation using machine learning," *Renew. Sustain. Energy Rev.*, vol. 82, pp. 2254–2269, Feb. 2018.

[18] B. Amrouche and X. L. Pivert, "Artificial neural network based daily local forecasting for global solar radiation," *Appl. Energy*, vol. 130, pp. 333–341, Oct. 2014.

[19] M. Deb and S. Roy, "Enhanced-pro: A new enhanced solar energy harvested prediction model for wireless sensor networks," *Wireless Pers. Commun.*, vol. 117, no. 2, pp. 1103–1121, Mar. 2021.

[20] J. C. López-Ardao, R. F. Rodriguez-Rubio, A. Suarez-Gonzalez, M. Rodriguez-Perez, and M. E. Sousa-Vieira, "Current trends on green wireless sensor networks," *Sensors*, vol. 21, no. 13, pp. 1–34, 2021.

[21] O. M. Gul and M. Demirekler, "Asymptotically throughput optimal scheduling for energy harvesting wireless sensor networks," *IEEE Access*, vol. 6, pp. 45004–45020, 2018.

[22] V. S. Rao, R. V. Prasad, and I. G. M. M. Niemegeers, "Optimal task scheduling policy in energy harvesting wireless sensor networks," in *Proc. IEEE Wireless Commun. Netw. Conf. (WCNC)*, New Orleans, LA, USA, Mar. 2015, pp. 1030–1035.

[23] L. Lei, Y. Kuang, X. S. Shen, K. Yang, J. Qiao, and Z. Zhong, "Optimal reliability in energy harvesting industrial wireless sensor networks," *IEEE Trans. Wireless Commun.*, vol. 15, no. 8, pp. 5399–5413, Aug. 2016.

[24] S. Kosunalp, "An energy prediction algorithm for wind-powered wireless sensor networks with energy harvesting," *Energy*, vol. 139, pp. 1275–1280, Nov. 2017.

[25] L. Li and C. Han, "ASARIMA: An adaptive harvested power prediction model for solar energy harvesting sensor networks," *Electronics*, vol. 11, no. 18, pp. 1–16, 2022.

[26] A. Cammarano, C. Petrioli, and D. Spenza, "Pro-energy: A novel energy prediction model for solar and wind energy-harvesting wireless sensor networks," in *Proc. IEEE 9th Int. Conf. Mobile Ad-Hoc Sensor Syst. (MASS)*, Las Vegas, NV, USA, Oct. 2012, pp. 75–83.

[27] M. Hiran and P. Kamboj, "Receiver-initiated energy harvesting MAC protocols: Survey," in *Proc. 3rd Int. Conf. Trends Electron. Informat. (ICOEI)*, Tirunelveli, India, Apr. 2019, pp. 1109–1115.

[28] H. H. R. Sherazi, L. A. Grieco, and G. Boggia, "A comprehensive review on energy harvesting MAC protocols in WSNs: Challenges and tradeoffs," *Ad Hoc Netw.*, vol. 71, pp. 117–134, Mar. 2018.

[29] H.-H. Lin, M.-J. Shih, H.-Y. Wei, and R. Vannithamby, "DeepSleep: IEEE 802.11 enhancement for energy-harvesting machine-to-machine communications," *Wireless Netw.*, vol. 21, no. 2, pp. 357–370, Feb. 2015.

[30] Y. Kim, C. W. Park, and T.-J. Lee, "MAC protocol for energy-harvesting users in cognitive radio networks," in *Proc. 8th Int. Conf. Ubiquitous Inf. Manage. Commun.*, Siem Reap, Cambodia, Jan. 2014, pp. 1–5.

[31] S. Sankpal and V. Bapat, "Performance evaluation of proposed SEHEE-MAC for wireless sensor network in habitat monitoring," *Int. J. Sci. Eng. Res.*, vol. 2, no. 10, pp. 1–6, 2011.

[32] J. Kim and J.-W. Lee, "Energy adaptive MAC for wireless sensor networks with RF energy transfer: Algorithm, analysis, and implementation," *Telecommun. Syst.*, vol. 64, no. 2, pp. 293–307, Feb. 2017.

[33] H.-H. Choi and W. Shin, "Harvest-until-access protocol based on slotted Aloha for wireless powered dense networks," in *Proc. Int. Conf. Electron., Inf., Commun. (ICEIC)*, Auckland, New Zealand, Jan. 2019, pp. 1–6.

[34] Y. Liu, Z. Yang, R. Yu, Y. Xiang, and S. Xie, "An efficient MAC protocol with adaptive energy harvesting for machine-to-machine networks," *IEEE Access*, vol. 3, pp. 358–367, 2015.

[35] S.-B. Lee, J.-H. Kwon, and E.-J. Kim, "Residual energy estimation-based MAC protocol for wireless powered sensor networks," *Sensors*, vol. 21, no. 22, pp. 1–21, 2021.

[36] S. Khan, A. N. Alvi, M. A. Javed, Y. D. Al-Otaibi, and A. K. Bashir, "An efficient medium access control protocol for RF energy harvesting based IoT devices," *Comput. Commun.*, vol. 171, pp. 28–38, Apr. 2021.

[37] M. Hawa, K. A. Darabkh, R. Al-Zubi, and G. Al-Sukkar, "A self-learning MAC protocol for energy harvesting and spectrum access in cognitive radio sensor networks," *J. Sensors*, vol. 2016, pp. 1–18, Mar. 2016.

[38] V. Esteves, A. Antonopoulos, E. Kartsakli, M. Puig-Vidal, P. Miribel-Català, and C. Verikoukis, "Cooperative energy harvesting-adaptive MAC protocol for WBANs," *Sensors*, vol. 15, no. 6, pp. 1–15, 2015.

[39] X. Fafoutis, A. Di Mauro, C. Orfanidis, and N. Dragoni, "Energy-efficient medium access control for energy harvesting communications," *IEEE Trans. Consum. Electron.*, vol. 61, no. 4, pp. 402–410, Nov. 2015.

[40] P. Kaur, P. Singh, and B. S. Sohi, "Adaptive MAC protocol for solar energy harvesting based wireless sensor networks in agriculture," *Wireless Pers. Commun.*, vol. 111, no. 4, pp. 2263–2285, Apr. 2020.

[41] Z. A. Eu and H.-P. Tan, "Probabilistic polling for multi-hop energy harvesting wireless sensor networks," in *Proc. IEEE Int. Conf. Commun. (ICC)*, Ottawa, ON, Canada, Jun. 2012, pp. 271–275.

[42] X. Fafoutis and N. Dragoni, "ODMAC: An on-demand MAC protocol for energy harvesting–wireless sensor networks," in *Proc. 8th ACM Symp. Perform. Eval. Wireless Ad Hoc, Sensor, Ubiquitous Netw.*, New York, NY, USA, Nov. 2011, pp. 49–56.

[43] H.-I. Liu, W.-J. He, and W. K. Seah, "LEB-MAC: Load and energy balancing MAC protocol for energy harvesting powered wireless sensor networks," in *Proc. 20th IEEE Int. Conf. Parallel Distrib. Syst. (ICPADS)*, Taiwan, Dec. 2014, pp. 584–591.

[44] K. Charoenchaiprakit, W. Piyarat, and K. Woradit, "Optimal data transfer of SEH-WSN node via MDP based on duty cycle and battery energy," *IEEE Access*, vol. 9, pp. 82947–82965, 2021.

[45] K. Nguyen, V.-H. Nguyen, D.-D. Le, Y. Ji, D. A. Duong, and S. Yamada, "ERI-MAC: An energy-harvested receiver-initiated MAC protocol for wireless sensor networks," *Int. J. Distrib. Sensor Netw.*, vol. 10, no. 5, pp. 1–8, 2014.

[46] D. Gao, S. Zhang, and F. Zhang, "HAS-MAC: A hybrid asynchronous and synchronous communication system for energy-harvesting wireless sensor networks," *Wireless Pers. Commun.*, vol. 119, no. 2, pp. 1743–1761, Mar. 2021.

[47] S. C. Kim, J. H. Jeon, and H. J. Park, "QoS aware energy-efficient (QAEE) MAC protocol for energy harvesting wireless sensor networks," in *Proc. Int. Conf. Hybrid Inf. Technol.*, Seoul, South Korea, 2012, pp. 41–48.

[48] J. Varghese and S. V. Rao, "Energy efficient exponential decision MAC for energy harvesting-wireless sensor networks," in *Proc. Int. Conf. Adv. Green Energy (ICAGE)*, Thiruvananthapuram, India, Dec. 2014, pp. 239–244.

[49] K. Shim and H.-K. Park, "Priority-based pipelined-forwarding MAC protocol for EH-WSNs," *Wireless Commun. Mobile Comput.*, vol. 2019, pp. 1–7, May 2019.

[50] T. N. Le, A. Pegatoquet, O. Berder, and O. Sentieys, "Energy-efficient power manager and MAC protocol for multi-hop wireless sensor networks powered by periodic energy harvesting sources," *IEEE Sensors J.*, vol. 15, no. 12, pp. 7208–7220, Dec. 2015.

[51] A. Obaid, M. Jaseemuddin, and X. Fernando, "An energy harvesting MAC protocol for cognitive wireless sensor networks," in *Proc. IEEE 93rd Veh. Technol. Conf. (VTC-Spring)*, Helsinki, Finland, Apr. 2021, pp. 1–6.

[52] S. Kosunalp, "EH-TDMA: A TDMA-based MAC protocol for energy-harvesting wireless sensor networks," *Int. J. Comput. Sci. Inf. Secur.*, vol. 14, no. 8, pp. 1–4, 2016.

[53] A. Bengheni, F. Didi, and I. Bambrik, "EEM-EHWSN: Enhanced energy management scheme in energy harvesting wireless sensor networks," *Wireless Netw.*, vol. 25, no. 6, pp. 3029–3046, Aug. 2019.

[54] T. D. Nguyen, J. Y. Khan, and D. T. Ngo, "An adaptive MAC protocol for RF energy harvesting wireless sensor networks," in *Proc. IEEE Global Commun. Conf. (GLOBECOM)*, Washington, DC, USA, Dec. 2016, pp. 1–6.

[55] S. Sarang, G. M. Stojanovic, M. Drieberg, S. Stankovski, and V. Jeoti, "Energy neutral operation based adaptive duty cycle MAC protocol for solar energy harvesting wireless sensor networks," in *Proc. IEEE 95th Veh. Technol. Conf. (VTC-Spring)*, Helsinki, Finland, Jun. 2022, pp. 1–6.

[56] S. Sarang, M. Drieberg, A. Awang, and R. Ahmad, "A QoS MAC protocol for prioritized data in energy harvesting wireless sensor networks," *Comput. Netw.*, vol. 144, pp. 141–153, Oct. 2018.

[57] R. Wang, W. Li, F. Gao, and T. Jiao, "The PSL MAC protocol for accumulated data processing in the energy-harvesting wireless sensor network," *Wireless Commun. Mobile Comput.*, vol. 2022, pp. 1–10, Jul. 2022.

[58] D. K. Sah, A. Hazra, R. Kumar, and T. Amgoth, "Harvested energy prediction technique for solar-powered wireless sensor networks," *IEEE Sensors J.*, early access, Sep. 28, 2022, doi: 10.1109/JSEN.2022.3208730.

[59] L. G. B. Ruiz, M. P. Cuéllar, M. D. Calvo-Flores, and M. D. C. P. Jiménez, "An application of non-linear autoregressive neural networks to predict energy consumption in public buildings," *Energies*, vol. 9, no. 9, pp. 1–21, 2016.

[60] *CC2420 Datasheet, TI*. Accessed: Dec. 16, 2022. [Online]. Available: http://www.ti.com/product/CC2420

[61] (Mar. 2022). *National Renewable Energy Laboratory*. Accessed: Dec. 2022. [Online]. Available: https://midcdmz.nrel.gov/oahu_archive/

[62] D. Benedetti, C. Petrioli, and D. Spenza, "GreenCastalia: An energy-harvesting-enabled framework for the Castalia simulator," in *Proc. 1st Int. Workshop Energy Neutral Sens. Syst.*, Rome, Italy, Nov. 2013, pp. 1–6.

[63] K. A. Ngo, T. T. Huynh, and D. T. Huynh, "Simulation wireless sensor networks in Castalia," in *Proc. Int. Conf. Intell. Inf. Technol.*, Hanoi, Vietnam, Feb. 2018, pp. 39–44.

[64] A. Varga. *OMNeT++: Discrete Event Simulator*. [Online]. Available: https://omnetpp.org

[65] Y. Ma, J. Guo, Y. Wang, A. Chakrabarty, H. Ahn, P. Orlik, X. Guan, and C. Lu, "Optimal dynamic transmission scheduling for wireless networked control systems," *IEEE Trans. Control Syst. Technol.*, vol. 30, no. 6, pp. 2360–2376, Nov. 2022.

[66] X. Huan, H. He, T. Wang, Q. Wu, and H. Hu, "A timestamp-free time synchronization scheme based on reverse asymmetric framework for practical resource-constrained wireless sensor networks," *IEEE Trans. Commun.*, vol. 70, no. 9, pp. 6109–6121, Sep. 2022.

[67] *IXOLAR High Efficiency*. Accessed: Sep. 18, 2022. [Online]. Available: https://www.digikey.com/en/product-highlight/i/ixys/ixolar-high-efficiency-solarmd-modules

[68] R. Han, W. Yang, Y. Wang, and K. You, "DCE: A distributed energy-efficient clustering protocol for wireless sensor network based on double-phase cluster-head election," *Sensors*, vol. 17, no. 5, pp. 1–15, 2017.

[69] M. Collotta, A. L. Cascio, G. Pau, and G. Scata, "A fuzzy controller to improve CSMA/CA performance in IEEE 802.15.4 industrial wireless sensor networks," in *Proc. IEEE 18th Conf. Emerg. Technol. Factory Autom. (ETFA)*, Cagliari, Italy, Sep. 2013, pp. 1–4.

[70] V. K. Garg and Y.-C. Wang, "Communication network architecture," in *The Electrical Engineering Handbook*. Burlington, VT, USA: Academic, 2005, pp. 989–1003.

[71] N. T. T. Hang, N. C. Trinh, N. T. Ban, M. Raza, and H. X. Nguyen, "Delay and reliability analysis of p-Persistent carrier sense multiple access for multi-event industrial wireless sensor networks," *IEEE Sensors J.*, vol. 20, no. 20, pp. 12402–12414, Oct. 2020.

[72] S. S. Alhajji and S. A. Alabady, "Slotted ALOHA based p-persistent CSMA energy-efficient MAC protocol for WSNs," *Int. J. Comput. Digit. Syst.*, vol. 10, no. 1, pp. 225–233, Feb. 2021.

[73] J. Shiraishi, A. E. Kalor, F. Chiariotti, I. Leyva-Mayorga, P. Popovski, and H. Yomo, "Query timing analysis for content-based wake-up realizing informative IoT data collection," *IEEE Wireless Commun. Lett.*, vol. 12, no. 2, pp. 327–331, Feb. 2023, doi: 10.1109/LWC.2022.3225333.

[74] J. Shiraishi, H. Yomo, K. Huang, C. Stefanovic, and P. Popovski, "Content-based wake-up for top-k query in wireless sensor networks," *IEEE Trans. Green Commun. Netw.*, vol. 5, no. 1, pp. 362–377, Mar. 2021.

[75] S. C. F. B. A. Forouzah, *Data Communications and Networking*, 4th ed. New York, NY, USA: McGraw-Hill, 2007.

[76] A. I. Al-Sulaifanie, S. Biswas, and B. K. Al-Sulaifanie, "AH-MAC: Adaptive hierarchical MAC protocol for low-rate wireless sensor network applications," *J. Sensors*, vol. 2017, pp. 1–16, Jan. 2017.

[77] G. Z. Papadopoulos, V. Kotsiou, A. Gallais, P. Chatzimisios, and T. Noël, "Wireless medium access control under mobility and bursty traffic assumptions in WSNs," *Mobile Netw. Appl.*, vol. 20, no. 5, pp. 649–660, Oct. 2015.

[78] M. M. Monowar, O. Rahman, A.-S. K. Pathan, and C. S. Hong, "Prioritized heterogeneous traffic-oriented congestion control protocol for WSNs," *Int. Arab J. Inf. Technol.*, vol. 9, no. 1, pp. 39–48, 2012.

[79] S. B. Nji, "Optimization of wireless body area networks for medical applications using the selective transmission algorithm," M.S. thesis, Faculty Eng., Comput. Sci., Swinburne Univ. Technol., Melbourne, VIC, Australia, 2017.
[80] N. Yamin and G. Bhat, "Online solar energy prediction for energy-harvesting Internet of Things devices," in *Proc. IEEE/ACM Int. Symp. Low Power Electron. Design (ISLPED)*, Boston, MA, USA, Jul. 2021, pp. 1–6.

SOHAIL SARANG (Graduate Student Member, IEEE) received the bachelor's degree in telecommunication engineering from Hamdard University, Karachi, Pakistan, in 2014, and the master's degree (by research) in electrical and electronics engineering from Universiti Teknologi PETRONAS (UTP), Malaysia, in 2018. He is currently pursuing the Ph.D. degree with the Faculty of Technical Sciences, University of Novi Sad (UNS), Serbia. He was engaged as a Marie Curie Early-Stage Researcher in AQUASENSE ITN Project, which received funding from the European Union's Horizon 2020 Research and Innovation Programme. His research interests include energy harvesting wireless sensor networks (EH-WSNs), the Internet of Things, medium access control (MAC) protocol, machine learning algorithms for EH-WSNs, and quality-of-service in sensor networks.

GORAN M. STOJANOVIĆ (Member, IEEE) received the B.Sc., M.Sc., and Ph.D. degrees in electrical engineering from the Faculty of Technical Sciences (FTS), University of Novi Sad (UNS), Novi Sad, Serbia, in 1996, 2003, and 2005, respectively. He is currently a Full Professor with FTS, UNS. He has authored 295 articles, including 136 in peer-reviewed journals with impact factors, five books, three patents, and one chapter in monograph. He is a keynote speaker for 12 international conferences and has over 17 years' experience in coordination of EU funded projects (Horizon Europe, H2020, EUREKA, ERASMUS, and CEI), with total budget exceeding 16.86 MEUR. His research interests include sensors, microfluidics, and flexible and textile electronics.

MICHEAL DRIEBERG (Member, IEEE) received the B.Eng. degree in electrical and electronics engineering from Universiti Sains Malaysia, Penang, Malaysia, in 2001, the M.Sc. degree in electrical and electronics engineering from Universiti Teknologi PETRONAS, Seri Iskandar, Malaysia, in 2005, and the Ph.D. degree in electrical and electronics engineering from Victoria University, Melbourne, Australia, in 2011. He is currently a Senior Lecturer with the Department of Electrical and Electronics Engineering, Universiti Teknologi PETRONAS. His research interests include radio resource management, medium access control protocols, energy harvesting communications, and performance analysis for wireless and sensor networks. He has published and served as a reviewer for several high impact journals and flagship conferences. He has also made several contributions to the wireless broadband standards group.

STEVAN STANKOVSKI (Member, IEEE) received the B.S. degree in electrical engineering from the Faculty of Technical Sciences, University of Novi Sad, in 1987, and the M.Sc. degree in computer science and automation and the Ph.D. degree in intelligent automated systems from the School of Electrical Engineering, University of Belgrade, in 1991 and 1994, respectively. He is currently a full-time Professor with the Mechatronics Department, University of Novi Sad. His research interests include mechatronics, artificial intelligence, and control systems. He has designed over a hundred different control systems and systems for supervision and control.

KISHORE BINGI (Member, IEEE) received the B.Tech. degree in electrical and electronics engineering from Acharya Nagarjuna University, India, in 2012, the M.Tech. degree in instrumentation and control systems from the National Institute of Technology, Calicut, India, in 2014, and the Ph.D. degree in electrical and electronic engineering from Universiti Teknologi PETRONAS, Malaysia, in 2019. From 2014 to 2015, he worked as an Assistant Systems Engineer at the TATA Consultancy Services Ltd., India. From 2019 to 2020, he worked as a Research Scientist and a Postdoctoral Researcher at the Universiti Teknologi PETRONAS. From 2020 to 2022, he served as an Assistant Professor at the Process Control Laboratory, School of Electrical Engineering, Vellore Institute of Technology, India. Since 2022, he has been working as a Faculty Member with the Department of Electrical and Electronic Engineering, Universiti Teknologi PETRONAS. His research interests include developing fractional-order neural networks, fractional-order systems and controllers, chaos prediction and forecasting, and advanced hybrid optimization techniques. He is an IET Member and a registered Chartered Engineer (C.Eng.) from Engineering Council U.K.

VARUN JEOTI (Senior Member, IEEE) received the Ph.D. degree from the Indian Institute of Technology, Delhi, India, in 1992. He has over 30 years of teaching experience in leading Indian and Malaysian universities teaching students from various social and cultural backgrounds. He has over 41 years of research and development experience. His research interests include signal processing, SAW sensor-tags, flexible and textile electronics, and wireless communication for various applications. He has supervised 18 Ph.D. students and 16 M.Sc. (by research) students. Starting in 1980, he was worked at IIT Delhi, soon after his graduation, he worked on various government sponsored projects at IIT Delhi and IIT Madras. Besides government grants, he has also secured industry grants valued about USD 4M. He is currently working with the Faculty of Technical Sciences, University of Novi Sad, Serbia, as the ERA Chair holder, leading research efforts in stretchable and textile electronics.